SF 298 MASTER COPY KEEP THIS COPY FOR REPRODUCTION PURPOSES

REPORT DOCUMENTATION PAGE

Form Approved OMB NO. 0704-0188

1. AGENCY USE ONLY *(Leave blank)*	2. REPORT DATE	3. REPORT TYPE AND DATES COVERED
	July 18, 1997	Final

4. TITLE AND SUBTITLE
Modeling, Identification, and Control Design for a Flexible Pointing System with Embedded Smart Materials

5. FUNDING NUMBERS
DAAH04-93-G-0209

6. AUTHOR(S)
Drs. F. Khorrami, S. U. Pillai, and S. Nourbakhsh

7. PERFORMING ORGANIZATION NAMES(S) AND ADDRESS(ES)
Polytechnic University
Six Metrotech Center
Brooklyn, New York 11201

8. PERFORMING ORGANIZATION REPORT NUMBER

9. SPONSORING / MONITORING AGENCY NAME(S) AND ADDRESS(ES)
U.S. Army Research Office
P.O. Box 12211
Research Triangle Park, NC 27709-2211

10. SPONSORING / MONITORING AGENCY REPORT NUMBER
ARO 32108.5-MA-SM

11. SUPPLEMENTARY NOTES
The views, opinions and/or findings contained in this report are those of the author(s) and should not be construed as an official Department of the Army position, policy or decision, unless so designated by other documentation.

12a. DISTRIBUTION / AVAILABILITY STATEMENT
Approved for public release; distribution unlimited.

12 b. DISTRIBUTION CODE

13. ABSTRACT *(Maximum 200 words)*

The research effort emphasized system identification, decentralized control design, and their applications to smart structures and flexible pointing systems. The research effort had both theoretical and experimental ingredients. On the theoretical side, new system identification techniques for nonrational systems, which may be either minimum phase or nonminimum phase, were developed. The identification techniques complemented our efforts on theoretical modeling of systems with embedded and/or surface mounted smart materials. . The advocated control strategies are decentralized and are robust to structured and unstructured perturbations of the system dynamics. This provides local decision making through the smart structures when multiple sensors and actuators are present. On the experimental side, we fabricated several smart composite tubes with piezoelectric sensors and actuators. One such tube (with surface mounted piezoceramic sensors and actuators) was used to replace part of the existing weapon pointing setup, namely ATB-1000, at the Army Research Laboratory at Picatinny Arsenal. Furthermore, we have developed similar experimental setups including a two-link flexible arm with piezoelectric sensors and actuators at the *Control/Robotics Research Laboratory (CRRL)* at Polytechnic.

14. SUBJECT TERMS	15. NUMBER IF PAGES
Decentralized Control, Adaptive Nonlinear Control, Smart Structures, Piezoceramic Actuators, System Identification	52
	16. PRICE CODE

17. SECURITY CLASSIFICATION OR REPORT	18. SECURITY CLASSIFICATION OF THIS PAGE	19. SECURITY CLASSIFICATION OF ABSTRACT	20. LIMITATION OF ABSTRACT
UNCLASSIFIED	UNCLASSIFIED	UNCLASSIFIED	UL

Final Report

Modeling, Identification, and Control Design for a Flexible Pointing System with Embedded Smart Materials

by

Farshad Khorrami, Principal Investigator

and

S. U. Pillai and S. Nourbakhsh, Co-Principal Investigators

Six Metrotech Center

Polytechnic University

Brooklyn, NY 11201

Summary of the Effort

The research effort emphasized system identification, decentralized control design, and their applications to smart structures and flexible pointing systems. The research effort had both theoretical and experimental ingredients. On the theoretical side, new system identification techniques for nonrational systems, which may be either minimum phase or nonminimum phase, were developed. The identification techniques complemented our efforts on theoretical modeling of systems with embedded and/or surface mounted smart materials. Having attained a theoretical model for systems at hand, robust linear and nonlinear control techniques are utilized for performance enhancement. The control strategies are robust to structured and unstructured perturbations of the system dynamics. The control design methodology are based on a decentralized framework. This provides local decision making through the smart structures when multiple sensors and actuators are present. On the experimental side, we fabricated several smart composite tubes with piezoelectric sensors and actuators. One such tube (with surface mounted piezoceramic sensors and actuators) was used to replace part of the existing weapon pointing setup, namely ATB-1000, at the Army Research Laboratory at Picatinny Arsenal. Furthermore, we have developed similar experimental setups including a two-link flexible arm with piezoelectric sensors and actuators at the *Control/Robotics Research Laboratory (CRRL)* at Polytechnic. The organization of the final report is as follows: a) the decentralized control design framework developed is reported first, b) the system identification for non-minimum phase systems is presented next, c) lastly a brief outline of our experimental effort is given.

Keywords: Nonlinear and Decentralized Control, Adaptive Control, System Identification, Non-minimum Phase Systems, Smart Structures.

Contents

1. Decentralized Adaptive Output Feedback Design for Large-Scale Nonlinear Systems

1.1 Introduction

Recently adaptive control techniques have been utilized for decentralized control of systems with uncertain interconnections bounded by first order polynomials[1–7]. The first available result on decentralized adaptive state feedback control for higher order interconnections was reported in [8]. A major structural restriction in [7,8] is that to ensure global stability, the interconnections must lie in the span of the input. Results on decentralized adaptive control for linear systems with subsystems having arbitrary relative degrees are presented in [1–4]. For higher order interconnections, the strict matching restriction was relaxed in [9], where decentralized adaptive state feedback controllers were designed using tools from centralized nonlinear control [10].

Relatively few results on decentralized output feedback are available in the literature, and still fewer for the adaptive case [5–7]. Recently, based on adaptive output feedback design in the centralized case [11], a decentralized adaptive regulator was designed for in [3] for systems of the observer canonical form. In all these output feedback schemes, the interconnections are assumed to be bounded by Lipschitz type bounds.

In this report, global decentralized adaptive output feedback controllers are designed for large scale nonlinear systems of the output feedback canonical form. We consider both parametric and dynamic uncertainties in the interconnections under the assumption that the interconnections are bounded by unknown pth order polynomials. In addition, we also consider bounded, unmeasurable disturbances entering the system. The design starts with the construction of decentralized filters for state estimation for each subsystem. The estimation error, however, is not exponentially convergent due to interconnections and disturbance terms. Utilizing techniques from [10,12], a systematic procedure is developed for design of an adaptive, decentralized controller which, through injection of nonlinear damping[1], guarantees global uniform boundedness of the tracking error and all the states of the closed-loop system to a compact set, and also provides good disturbance rejection properties. The size of the compact set can be made arbitrarily small through proper choice of the control gains. A higher order composite Lyapunov function is employed to prove global decentralized stabilization. Furthermore, while the majority of output feedback schemes in the centralized case can handle only linear parametric uncertainties, the proposed scheme incorporates both parametric and dynamic uncertainties in the interconnections, and the uncertain parameters may appear nonlinearly in the vector fields. In addition, the

[1]The nonlinear damping terms designed in this report are different from those obtained by Kanellakopoulos *et. al* [10].

proposed scheme requires adaptation of only one scalar parameter for each channel in contrast to [11], where the number of adaptations is the same as the number of uncertain parameters. Furthermore, no controller redesign is required if additional subsystems are brought on-line or taken off-line. Global asymptotic properties are attained for the case where the objective is regulation.

1.2 The Class of Large-Scale Nonlinear Systems

We consider a large-scale continuous time affine nonlinear system comprised of N channels (agents) given by

$$\begin{aligned} \dot{x} &= f(x) + \sum_{i=1}^{N} g_i(x)u_i + p(x)\omega(t) \\ y_j &= h_j(x) \quad 1 \le j \le N \end{aligned} \tag{1.1}$$

where $x \in \mathcal{R}^n$ is the state vector for the overall system, $u_i \in \mathcal{R}$ and $y_i \in \mathcal{R}$ are the input and output for the ith subsystem, and $\omega(t)$ is a bounded unmeasurable disturbance signal. The vector fields f, p, g_i, and the function h_j are assumed to be smooth on $\mathcal{R}^n$, with $f(0) = 0$, $p(0) = 0$, $h_j(0) = 0$, and $g_i(0) \neq 0$. Only the output y_i is available for feedback to the ith control channel.

The decentralized scheme proposed in this report is applicable to a class of large-scale nonlinear systems which are transformable via a global diffeomorphism

$$z = [z_{11} \dots z_{1\kappa_1} z_{12} \dots z_{N1} \dots z_{N\kappa_N}]^T = \Phi(x); \quad \Phi(0) = 0$$

into the output-feedback canonical form:

$$\begin{aligned} \dot{z}_{i1} &= z_{i2} + \varphi_{i1}(y_1 \dots y_N) + \xi_{i1}(y_1 \dots y_N)\omega(t) \\ &\vdots \\ \dot{z}_{i,\rho_i-1} &= z_{i,\rho_i} + \varphi_{i,\rho_i-1}(y_1 \dots y_N) + \xi_{i,\rho_i-1}(y_1 \dots y_N)\omega(t) \\ \dot{z}_{i,\rho_i} &= z_{i,\rho_i+1} + \varphi_{i,\rho_i}(y_1 \dots y_N) + \xi_{i,\rho_i}(y_1 \dots y_N)\omega(t) + b_{i,\kappa_i-\rho_i}\delta_i(y_i)u_i \\ &\vdots \\ \dot{z}_{i,\kappa_i} &= \varphi_{i,\kappa_i}(y_1 \dots y_N) + \xi_{i,\kappa_i}(y_1 \dots y_N)\omega(t) + b_{i0}\delta_i(y_i)u_i \\ y_i &= z_{i1}, \quad 1 \le i \le N \end{aligned} \tag{1.2}$$

where κ_i, $1 \le i \le N$ are the observability indices with $\kappa_1 \ge \kappa_2 \ge \cdots \ge \kappa_N \ge 1$ and $\sum_{i=1}^{N} \kappa_i = N$, and $b_{i,\kappa_i-\rho_i} \dots b_{i0}$ are unknown constant parameters. The coordinate-free necessary and conditions for transformation of (1.1) to (1.2) are given in [14].

We consider both parametric and dynamic uncertainties in the terms $\varphi_{ij}(y_1 \dots y_N)$ and $\xi_{ij}(y_1 \dots y_N)$, $1 \le i \le N$, $1 \le j \le \kappa_i$. Specifically, we assume that φ_{ij}, ξ_{ij} are unknown except that they are bounded by an unknown p_{ij}th order polynomial in outputs, i.e.,

$$\|\varphi_{ij}(y_1 \dots y_N)\| \leq \sum_{k=0}^{p_{ij}} \sum_{l=1}^{N} \zeta_{ijl}^k \|y_l\|^k; \qquad \|\xi_{ij}(y_1 \dots y_N)\| \leq \sum_{k=0}^{p_{ij}} \sum_{l=1}^{N} \nu_{ijl}^k \|y_l\|^k \tag{1.3}$$

with ζ_{ijl}^k and ν_{ijl}^k unknown.

Remark 2.1: Note that φ_{ij} and ξ_{ij} may be nonlinearly parameterized in the unknown parameters provided condition (1.3) is satisfied. Also, only the quantity $p = \max_{1\leq i\leq N;\ 1\leq j\leq \kappa_i} p_{ij}$ needs to be known.

To avoid losing insight of the underlying idea of this report, we assume that the parameters b_{ij}, $0 \leq j \leq \kappa_i - \rho_i$, $1 \leq i \leq N$, are known. The case of unknown b_{ij} can be treated identically as in [11] where the following assumptions are made:

Assumption (2.1): The sign of $b_{i,\kappa_i-\rho_i}$ is known.

Assumption (2.2): The polynomial $B_i(s) = b_{i,\kappa_i-\rho_i} s^{\kappa_i-\rho_i} + \cdots + b_{i1}s + b_{i0}$ is strict Hurwitz (exponential stability of the zero dynamics).

Assumption (2.3): $\delta_i(y_i) \neq 0$,

Assumption (2.4): The reference signal $y_{i,ref}$ and its first ρ_i derivatives are known and bounded with $y_{i,ref}^{(\rho_i)}$ piecewise continuous.

For known b_{ij}, we assume assumptions (2.2), (2.3), and (2.4) to be true.

1.3 Decentralized Adaptive Design

The decentralized adaptive control scheme is designed for the transformed system (1.2). Since only the ith output (y_i) can be utilized for feedback to ith control channel (u_i), we need to design an observer to estimate the remaining states of the ith subsystem. However, an observer with linearizable error dynamics cannot be designed in this case due to parametric and dynamic uncertainties in the φ_{ij} terms in (1.2). Even if the exact form of φ_{ij} is known, in the decentralized context, the presence of unmeasurable outputs from other subsystems y_k, $1 \leq k \leq N; k \neq i$ makes it impossible to obtain a linearized error dynamics. However, as will be shown in the ensuing design procedure, the observer error can still be made to converge to zero asymptotically using nonlinear damping terms in the control. The systematic design procedure presented here employs tools from the nonlinear design toolkit by Kanellakopoulos et al.[10].

The ith subsystem (1.2) can be written as:

$$\dot{z}_i = A_i z_i + k_i y_i + \varphi_i(y_1 \dots y_N) + \xi_i(y_1 \dots y_N)\omega(t) + b_i \delta_i(y_i) u_i \tag{1.4}$$

where

$$A_i = \begin{bmatrix} -k_{i1} & & \\ \vdots & & I \\ -k_{i,\kappa_i} & 0 \ \cdots \ 0 & \end{bmatrix}, \quad k_i = \begin{bmatrix} k_{i1} \\ \vdots \\ k_{i,\kappa_i} \end{bmatrix}, \quad b_i^T = \begin{bmatrix} 0 & \cdots & 0 & b_{i,\kappa_i-\rho_i} & \cdots & b_{i0} \end{bmatrix},$$

$$\varphi_i^T = \begin{bmatrix} \varphi_{i1} & \cdots & \varphi_{i,\kappa_i} \end{bmatrix}, \quad \xi_i^T = \begin{bmatrix} \xi_{i1} & \cdots & \xi_{i,\kappa_i} \end{bmatrix}.$$

The gains k_i are chosen such that A_i is a strict Hurwitz matrix.
We define the estimate of the states z_i as

$$\dot{\hat{z}}_i = A_i\hat{z}_i + k_i y_i + b_i\delta_i(y_i)u_i. \tag{1.5}$$

The observer error $\epsilon_i = z_i - \hat{z}_i$ is given by

$$\dot{\epsilon}_i = A_i\epsilon + \varphi_i(y_1 \dots y_N) + \xi_i(y_1 \dots y_N)\omega(t). \tag{1.6}$$

Since A_i is a strict Hurwitz matrix, given a positive definite matrix Q_i, there exists a positive definite solution P_i to the Lyapunov equation

$$A_i^T P_i + P_i A_i = -Q_i. \tag{1.7}$$

In the following, we assume uniform relative degree for each subsystem ($\rho_i = \rho$, $1 \leq i \leq N$) in order to reduce notational complexity. The case where the relative degrees are different for each subsystem can be treated similarly.
The ensuing systematic design procedure involves at each step, augmenting an integrator and the design of a *virtual* control law to stabilize the augmented system, until the actual control appears at the ρth step.
Step 0: Define the tracking error for the ith subsystem as $\chi_{i1} = z_{i1} - y_{i,ref} \triangleq y_i - \tau_{i0}(y_{i,ref})$. Expressing z_{i2} in terms of its estimate as $z_{i2} = \hat{z}_{i2} + \epsilon_{i2}$, we obtain

$$\dot{\chi}_{i1} = \hat{z}_{i2} + \varphi_{i1}(y_1 \dots y_N) + \xi_{i1}(y_1 \dots y_N)\omega(t) - \dot{y}_{i,ref} + \epsilon_{i2}, \quad 1 \leq i \leq N. \tag{1.8}$$

The following *virtual* decentralized control law $\hat{z}_{i2}$ for the ith subsystem (1.8) is proposed

$$\hat{z}_{i2} = -\pi_{i1}\chi_{i1} - \hat{\beta}_i\chi_{i1} - \gamma_i\varrho_i(\chi_{i1} + \chi_{i1}^{2p-1}) + \dot{y}_{i,ref} \triangleq \tau_{i1}(\chi_{i1}, \hat{\beta}_i) + \dot{y}_{i,ref} \tag{1.9}$$

where $\varrho_i > 0$, $\hat{\beta}_i$ is a time varying adaptation gain to counter the effects of the interconnections, π_{i1} is a constant gain whose magnitude will determine the ultimate bound on the tracking error, and γ_i is a constant gain given by

$$\gamma_i = (\frac{1}{2} + Np_{i1})\sum_{k=1}^{p} k^2 = \frac{(1 + 2Np_{i1})p(p+1)(2p+1)}{12}. \tag{1.10}$$

Since $\hat{z}_{i2}$ is not the actual control, define:

$$\chi_{i2} = \hat{z}_{i2} - \tau_{i1}(\chi_{i1}, \hat{\beta}_i) - \dot{y}_{i,ref}. \tag{1.11}$$

Therefore, $\dot{\chi}_{i1} = \chi_{i2} + \tau_{i1}(\chi_{i1}, \hat{\beta}_i) + \varphi_{i1}(y_1 \dots y_N) + \xi_{i1}(y_1 \dots y_N)\omega(t) + \epsilon_{i2}$.
Let β_i^* be the desired value of the control gain $\hat{\beta}_i$ to counteract the effects of the interconnections. The following adaptation for $\hat{\beta}_i$ is used

$$\dot{\hat{\beta}}_i = \Gamma_i\varrho_i\sum_{k=1}^{p} k\chi_{i1}^{2k} - \sigma_i\Gamma_i\hat{\beta}_i \tag{1.12}$$

where $\sigma_i > 0$ incorporates the standard "σ modification" used in robust adaptive control to avoid parameter drift. The true value of β_i^* required to counter the effects of the interconnections is obtained in the final step.
Consider the following composite Lyapunov function for the sub-subsystems (1.8)

$$V_0 = \sum_{i=1}^{N} \left\{ \epsilon_i^T P_i \epsilon_i + \sum_{k=1}^{p} \varrho_i \chi_{i1}^{2k} + \Gamma_i^{-1} (\hat{\beta}_i - \beta_i^*)^2 \right\} \tag{1.13}$$

where Γ_i is a positive constant. Differentiating V_0 along the trajectories of χ_{i1}, we obtain

$$\begin{aligned}
\dot{V}_0 = \sum_{i=1}^{N} \Bigg\{ & -\epsilon_i^T Q_i \epsilon_i + 2\epsilon_i^T P_i \left(\varphi_i(y_1 \dots y_N) + \xi_i(y_1 \dots y_N)\omega(t)\right) + \sum_{k=1}^{p} 2k\varrho_i \chi_{i1}^{2k-1} [\chi_{i2} \\
& + \tau_{i1}(\chi_{i1}, \hat{\beta}_i) + \epsilon_{i2} + \varphi_{i1}(y_1 \dots y_N) + \xi_{i1}(y_1 \dots y_N)\omega(t)] + 2\Gamma_i^{-1}(\hat{\beta}_i - \beta_i^*)\dot{\hat{\beta}}_i \Bigg\} \\
\leq \sum_{i=1}^{N} \Big\{ & -\lambda_{min}(Q_i)\|\epsilon_i\|^2 + 2\|\epsilon_i\|\|P_i\| \left(\|\varphi_i(y_1 \dots y_N)\| + \|\xi_i(y_1 \dots y_N)\omega(t)\|\right) \\
& - 2\pi_{i1}\varrho_i \sum_{k=1}^{p} \chi_{i1}^{2k} + \sum_{k=1}^{p} 2k\varrho_i \chi_{i1}^{2k-1} [\chi_{i2} - \gamma_i \varrho_i (\chi_{i1} + \chi_{i1}^{2p-1}) - \beta_i^* \chi_{i1} + \epsilon_{i2}] \\
& + \sum_{k=1}^{p} 2k\varrho_i \|\chi_{i1}\|^{2k-1} \{\|\varphi_{i1}(y_1 \dots y_N)\| + \|\xi_{i1}(y_1 \dots y_N)\omega(t)\|\} \\
& + 2(\hat{\beta}_i - \beta_i^*)\{\Gamma_i^{-1}\dot{\hat{\beta}}_i - \varrho_i \sum_{k=1}^{p} k\chi_{i1}^{2k}\} \Big\}.
\end{aligned} \tag{1.14}$$

Utilizing the bounds (1.3) and inequalities

$$2ab \leq a^2 + b^2; \tag{1.15}$$

$$\left(\sum_{k=1}^{p} a_k b_k \right)^2 \leq \left(\sum_{k=1}^{p} a_k^2 \right) \left(\sum_{k=1}^{p} b_k^2 \right); \tag{1.16}$$

$$\left\{ \sum_{i=1}^{2} |a_i| \right\}^k \leq 2^k \sum_{i=1}^{2} |a_i|^k, \tag{1.17}$$

the terms in (1.14) can be bounded as

$$\begin{aligned}
\sum_{i=1}^{N} \sum_{k=1}^{p} 2k\varrho_i \|\chi_{i1}\|^{2k-1} \|\varphi_{i1}(y_1 \dots y_N)\| & \leq \sum_{i=1}^{N} \sum_{k=1}^{p} 2k\varrho_i \|\chi_{i1}\|^{2k-1} \sum_{k_1=1}^{p_{i1}} \sum_{j=1}^{N} \zeta_{i1j}^{k_1} \|y_j\|^{k_1} \quad \text{(Using (1.3))} \\
= \sum_{i=1}^{N} \sum_{k_1=1}^{p_{i1}} \sum_{j=1}^{N} 2 & \left\{ \sum_{k=1}^{p} k\varrho_i \|\chi_{i1}\|^{2k-1} \right\} \zeta_{i1j}^{k_1} \|y_j\|^{k_1}
\end{aligned}$$

$$\leq \sum_{i=1}^{N}\sum_{k_1=1}^{p_{i1}}\sum_{j=1}^{N}\left\{\left(\sum_{k=1}^{p} k\varrho_i\|\chi_{i1}\|^{2k-1}\right)^2+\left(\zeta_{i1j}^{k_1}\right)^2\|y_j\|^{2k_1}\right\}\quad\text{(Using (1.15))}$$

$$\leq \sum_{i=1}^{N}\sum_{k_1=1}^{p_{i1}}\sum_{j=1}^{N}\{\sum_{k=1}^{p}k^2\varrho_i^2\}\{\sum_{k=1}^{p}\|\chi_{i1}\|^{4k-2}\}+\sum_{i=1}^{N}\sum_{k=1}^{p_{i1}}d_{1ik}(\|y_{j,ref}\|+\|\chi_{i1}\|)^{2k}$$

$$\text{(Using (1.16))};\ \ d_{1ik}=\sum_{j=1}^{N}\left(\zeta_{j1i}^{k}\right)^2$$

$$\leq \sum_{i=1}^{N}\gamma_{i1}\varrho_i^2\sum_{k=1}^{p}\|\chi_{i1}\|^{4k-2}+\sum_{i=1}^{N}\sum_{k=1}^{p_{i1}}2^{2k}d_{1ik}\|y_{i,ref}\|^{2k}+\sum_{i=1}^{N}\sum_{k=1}^{p}2^{2k}d_{1ik}\|\chi_{i1}\|^{2k}\qquad(1.18)$$

$$\text{(Using (1.17))};\ \ \gamma_{i1}=Np_{i1}\sum_{k=1}^{p}k^2=\frac{Np_{i1}p(p+1)(2p+1)}{6}.$$

Similarly,

$$\sum_{i=1}^{N}\sum_{k=1}^{p}2k\varrho_i\|\chi_{i1}\|^{2k-1}\|\xi_{i1}(y_1\ldots y_N)\omega(t)\|$$

$$\leq \sum_{i=1}^{N}\gamma_{i1}\varrho_i^2\sum_{k=1}^{p}\|\chi_{i1}\|^{4k-2}+\sum_{i=1}^{N}\sum_{k=1}^{p_{i1}}2^{2k}\upsilon_{1ik}\|y_{i,ref}\|^{2k}+\sum_{i=1}^{N}\sum_{k=1}^{p}2^{2k}\upsilon_{1ik}\|\chi_{i1}\|^{2k}\qquad(1.19)$$

$$\text{with } \gamma_{i1} \text{ as in (1.18)};\ \ \upsilon_{1ik}=\sum_{j=1}^{N}\left(\omega_{max}\nu_{j1i}^{k}\right)^2,$$

$$\sum_{i=1}^{N}\sum_{k=1}^{p}2k\varrho_i\chi_{i1}^{2k-1}\epsilon_{i2}\leq\sum_{i=1}^{N}2\left\{\sum_{k=1}^{p}k\varrho_i\|\chi_{i1}\|^{2k-1}\right\}\|\epsilon_i\|$$

$$\leq \sum_{i=1}^{N}\frac{\varrho_i^2}{6}p(p+1)(2p+1)\sum_{k=1}^{p}\|\chi_{i1}\|^{4k-2}+\sum_{i=1}^{N}\|\epsilon_i\|^2,\qquad(1.20)$$

$$\sum_{i=1}^{N}2\|\epsilon_i\|\left(\|P_i\|\|\varphi_i(y_1\ldots y_N)\|\right)\leq\sum_{i=1}^{N}\|\epsilon_i\|^2+\sum_{i=1}^{N}\|P_i\|^2\|\varphi_i(y_1\ldots y_N)\|^2$$

$$\leq \sum_{I=1}^{N}\|\epsilon_i\|^2+\sum_{i=1}^{N}\sum_{j=1}^{\kappa_i}\|P_i\|^2\|\varphi_{ij}(y_1\ldots y_N)\|^2$$

$$\leq \sum_{i=1}^{N}\|\epsilon_i\|^2+\sum_{i=1}^{N}\sum_{j=1}^{\kappa_i}\sum_{k=1}^{p_{ij}}\sum_{l=1}^{N}\|P_i\|^2\left(\zeta_{ijl}^{k}\right)^2\|y_l\|^{2k}\quad\text{(Using (1.17))}$$

$$\leq \sum_{i=1}^{N}\|\epsilon_i\|^2+\sum_{i=1}^{N}\sum_{k=1}^{p}d_{ik}\|y_i\|^{2k};\quad\text{where } d_{ik}=\sum_{l=1}^{N}\|P_l\|^2\sum_{j=1}^{\kappa_l}\left(\zeta_{lji}^{k}\right)^2$$

$$\leq \sum_{i=1}^{N}\|\epsilon_i\|^2+\sum_{i=1}^{N}\sum_{k=1}^{p}2^{2k}d_{ik}\|y_{i,ref}\|^{2k}+\sum_{i=1}^{N}\sum_{k=1}^{p}2^{2k}d_{ik}\|\chi_{i1}\|^{2k}, \tag{1.21}$$

$$\sum_{i=1}^{N}2\|\epsilon_i\|\left(\|P_i\|\|\xi_i(y_1\dots y_N)\omega(t)\|\right)\leq\sum_{i=1}^{N}\|\epsilon_i\|^2+\sum_{i=1}^{N}\sum_{k=1}^{p}2^{2k}\upsilon_{ik}\|y_{i,ref}\|^{2k}$$
$$+\sum_{i=1}^{N}\sum_{k=1}^{p}2^{2k}\upsilon_{ik}\|\chi_{i1}\|^{2k};\quad \upsilon_{ik}=\sum_{l=1}^{N}\|P_l\|^2\sum_{j=1}^{\kappa_l}\left(\omega_{max}\nu_{lji}^{k}\right)^2. \tag{1.22}$$

With adaptation (1.12) and utilizing the bounds (1.18)-(1.22), and noting that $\gamma_i=\gamma_{i1}+\frac{1}{2}\sum_{k=1}^{p}k^2$, $\dot{V}_0$ may be written as

$$\dot{V}_0\leq\sum_{i=1}^{N}\Bigg\{-\{\lambda_{min}(Q_i)-3\}\|\epsilon_i\|^2-2\pi_{i1}\varrho_i\sum_{k=1}^{p}\chi_{i1}^{2k}+\sum_{k=1}^{p}2k\varrho_i\chi_{i1}^{2k-1}\chi_{i2}$$
$$+2\gamma_i\varrho_i^2\sum_{k=1}^{p}\|\chi_{i1}\|^{4k-2}-2\gamma_i\varrho_i^2(\chi_{i1}+\chi_{i1}^{2p-1})\sum_{k=1}^{p}\chi_{i1}^{2k-1}-2\sigma_i(\hat{\beta}_i-\beta_i^*)\hat{\beta}_i$$
$$+\sum_{k=1}^{p}2^{2k}(d_{ik}+\upsilon_{ik}+d_{1ik}+\upsilon_{1ik})(\|\chi_{i1}\|^{2k}+\|y_{i,ref}\|^{2k})-2\beta_i^*\varrho_i\sum_{k=1}^{p}k\chi_{i1}^{2k}\Bigg\} \tag{1.23}$$
$$\leq\sum_{i=1}^{N}\Bigg\{-\{\lambda_{min}(Q_i)-3\}\|\epsilon_i\|^2-2\pi_{i1}\varrho_i\sum_{k=1}^{p}\chi_{i1}^{2k}+\sum_{k=1}^{p}2k\varrho_i\chi_{i1}^{2k-1}\chi_{i2}-\sigma_i(\hat{\beta}_i-\beta_i^*)^2$$
$$+\sigma_i\beta_i^{*2}+\sum_{k=1}^{p}2^{2k}(d_{ik}+\upsilon_{ik}+d_{1ik}+\upsilon_{1ik})(\|\chi_{i1}\|^{2k}+\|y_{i,ref}\|^{2k})-2\beta_i^*\varrho_i\sum_{k=1}^{p}k\chi_{i1}^{2k}\Bigg\} \tag{1.24}$$

Inequality (1.24) is obtained from (1.23) by completing squares of the $(\hat{\beta}_i-\beta_i^*)$ terms and using the fact that the resultant of the first two terms in the second line of (1.23) is negative.

The state equations for χ_{i1}, χ_{i2} are given by

$$\begin{aligned}
\dot{\chi}_{i1} &= \chi_{i2}+\tau_{i1}(\chi_{i1},\hat{\beta}_i)+\varphi_{i1}(y_1\dots y_N)+\xi_{i1}(y_1\dots y_N)\omega(t)+\epsilon_{i2}\\
\dot{\chi}_{i2} &= \hat{z}_{i3}+k_{i2}(y_i-\hat{z}_{i1})-\frac{\partial\tau_{i1}}{\partial\chi_{i1}}\{\chi_{i2}+\tau_{i1}(\chi_{i1},\hat{\beta}_i)\}-\frac{\partial\tau_{i1}}{\partial\hat{\beta}_i}\dot{\hat{\beta}}_i-\ddot{y}_{i,ref}\\
&\quad-\frac{\partial\tau_{i1}}{\partial\chi_{i1}}\{\varphi_{i1}(y_1\dots y_N)+\xi_{i1}(y_1\dots y_N)\omega(t)+\epsilon_{i2}\}\\
&= \hat{z}_{i3}+\varsigma_{i2}(y_i,\hat{z}_{i1},\hat{z}_{i2},\hat{\beta}_i,y_{i,ref},\dot{y}_{i,ref},\ddot{y}_{i,ref})\\
&\quad+\varpi_{i2}(\chi_{i1},\hat{\beta}_i)\{\epsilon_{i2}+\varphi_{i1}(y_1\dots y_N)+\xi(y_1\dots y_N)\omega(t)\}.
\end{aligned} \tag{1.25}$$

Remark 3.1: The terms $(d_{1ik}+\upsilon_{i1k})\|\chi_{i1}\|^{2k}$ in $\dot{V}_0$ arise due to the interconnection and disturbance terms appearing in the state equations of the plant (see e.g., (1.8), (1.25)). However, as can be seen from (1.24), these terms are in the span of the control

and can be countered using sufficiently high control gain β_i^*. In the subsequent steps, additional terms of the type $(.)\|\chi_{i1}\|^{2k}$ will appear due to disturbance and interconnections. The desired value of β_i^* to counter these effects is assigned in the final step. Similarly, possibly destabilizing disturbance and interconnection terms arise in the observer error dynamics (1.6). These appear as $(d_{ik} + \upsilon_{ik})\|\chi_{i1}\|^{2k}$ in the Lyapunov function and can again be countered by injecting nonlinear damping through β_i^*.

The design procedure can now be made recursive as shown in the following step:

Step m ($1 \leq m \leq \rho - 2$): In steps 0 to $m-1$, the virtual controls $\tau_{i1} \ldots \tau_{i,m}$ were designed. In the $m-1$th step, $\chi_{i,m+1}$ is defined as the difference of $\hat{z}_{i,m+1}$ and $\tau_{i,m}$, i.e.,

$$\chi_{i,m+1} = \hat{z}_{i,m+1} - \tau_{im}(y_i, \hat{z}_{i1} \ldots \hat{z}_{i,m}, \hat{\beta}_i, y_{i,ref} \ldots y_{i,ref}^{(m)}), \tag{1.26}$$

The dynamics for $\chi_{i,m+1}$ are given by

$$\begin{aligned}\dot{\chi}_{i,m+1} &= \hat{z}_{i,m+2} + \varsigma_{i,m+1}(y_i, \hat{z}_{i1} \ldots \hat{z}_{i,m+1}, \hat{\beta}_i, y_{i,ref} \ldots y_{i,ref}^{(m+1)}) \\ &+\varpi_{i,m+1}(y_i, \hat{z}_{i1} \ldots \hat{z}_{i,m+1}, \hat{\beta}_i, y_{i,ref} \ldots y_{i,ref}^{(m+1)})\{\epsilon_{i2} + \varphi_{i1}(y_1 \ldots y_N) \\ &+\xi_{i1}(y_1 \ldots y_N)\omega(t)\}\end{aligned} \tag{1.27}$$

where the notation in (1.27) is similar to that used in (1.25). We consider $\hat{z}_{i,m+2}$ as the virtual control for the $(\chi_{i1} \ldots \chi_{i,m+1})$ sub-subsystems and use the following composite Lyapunov function for this subsystem:

$$V_m = V_{m-1} + \sum_{i=1}^{N} \chi_{i,m+1}^2. \tag{1.28}$$

Differentiating along the trajectories of $(\chi_{i1} \ldots \chi_{i,m+1})$, we obtain

$$\begin{aligned}\dot{V}_m \leq \sum_{i=1}^{N} \Bigg[& -\{\lambda_{min}(Q_i) - (m+2)\}\|\epsilon_i\|^2 - \sigma_i(\hat{\beta}_i - \beta_i^*)^2 - 2\pi_{i1}\varrho_i \sum_{k=1}^{p} \chi_{i1}^{2k} - 2\sum_{j=2}^{m} \pi_{ij}\chi_{ij}^2 \\ & +2\chi_{i,m+1}\left\{\hat{z}_{i,m+2} + \chi_{im} + \varsigma_{i,m+1}(y_i, \hat{z}_{i1} \ldots \hat{z}_{i,m+1}, \hat{\beta}_i, y_{i,ref} \ldots y_{i,ref}^{(m+1)})\right\} \\ & +2\chi_{i,m+1}\varpi_{i,m+1}(y_i, \hat{z}_{i1} \ldots \hat{z}_{i,m+1}, \hat{\beta}_i, y_{i,ref} \ldots y_{i,ref}^{(m+1)}) \\ & \{\epsilon_{i2} + \varphi_{i1}(y_1 \ldots y_N) + \xi_{i1}(y_1 \ldots y_N)\omega(t)\} \\ & + \sum_{k=1}^{p} 2^{2k}\{d_{ik} + \upsilon_{ik} + m(d_{1ik} + \upsilon_{1ik})\}\{\|\chi_{i1}\|^{2k} + \|y_{i,ref}\|^{2k}\} \\ & +\sigma_i\beta_i^{*2} - 2\beta_i^*\varrho_i \sum_{k=1}^{p} k\chi_{i1}^{2k}\Bigg].\end{aligned} \tag{1.29}$$

Note that for $m = 1$, instead of the term $2\chi_{i2}\chi_{i1}$ in (1.29), we have $2\chi_{i2}\sum_{k=1}^{p} k\varrho_i\chi_{i1}^{2k-1}$. Utilizing bounds (1.3) and inequalities (1.15)-(1.17), the terms in (1.29) may be bounded as

$$\sum_{i=1}^{N} 2\chi_{i,m+1}\varpi_{i,m+1}\epsilon_{i2} \leq \sum_{i=1}^{N} \chi_{i,m+1}^2\varpi_{i,m+1}^2 + \|\epsilon_i\|^2, \tag{1.30}$$

$$\begin{aligned}\sum_{i=1}^{N} 2\chi_{i,m+1}\varpi_{i,m+1}\varphi_{i1}(y_1 \dots y_N) &\leq \sum_{i=1}^{N} \chi_{i,m+1}^2\varpi_{i,m+1}^2 + \sum_{i=1}^{N}\sum_{j=1}^{N}\sum_{k=1}^{p_{i1}} \left(\zeta_{ij1}^k\right)^2 \|y_j\|^{2k} \\ &\leq \sum_{i=1}^{N} \chi_{i,m+1}^2\varpi_{i,m+1}^2 + \sum_{i=1}^{N}\sum_{k=1}^{p_{i1}} 2^{2k} d_{1ik}\|y_{i,ref}\|^{2k} + \sum_{i=1}^{n}\sum_{k=1}^{p} 2^{2k} d_{1ik}\|\chi_{i1}\|^{2k}, \end{aligned} \tag{1.31}$$

$$\begin{aligned}&\sum_{i=1}^{N} 2\chi_{i,m+1}\varpi_{i,m+1}\xi_{i1}(y_1 \dots y_N)\omega(t) \\ &\leq \sum_{i=1}^{N} \chi_{i,m+1}^2\varpi_{i,m+1}^2 + \sum_{i=1}^{N}\sum_{k=1}^{p_{i1}} 2^{2k} \upsilon_{1ik}\|y_{i,ref}\|^{2k} + \sum_{i=1}^{n}\sum_{k=1}^{p} 2^{2k} \upsilon_{1ik}\|\chi_{i1}\|^{2k} \end{aligned} \tag{1.32}$$

where d_{1ik}, υ_{1ik} are as in (1.18) and (1.19). Using (1.30)-(1.32), $\dot{V}_m$ is written as

$$\begin{aligned}\dot{V}_m \leq \sum_{i=1}^{N} \Bigg[& -\{\lambda_{min}(Q_i) - (m+3)\}\|\epsilon_i\|^2 - \sigma_i(\hat{\beta}_i - \beta_i^*)^2 - 2\pi_{i1}\varrho_i \sum_{k=1}^{p} \chi_{i1}^{2k} - 2\sum_{j=2}^{m} \pi_{ij}\chi_{ij}^2 \\ & +2\chi_{i,m+1}\{\hat{z}_{i,m+2} + \chi_{im} + \varsigma_{i,m+1}(y_i, \hat{z}_{i1} \dots \hat{z}_{i,m+1}, \hat{\beta}_i, y_{i,ref} \dots y_{i,ref}^{(m+1)}) \\ & +\chi_{i,m+1}\varpi_{i,m+1}^2(y_i, \hat{z}_{i1} \dots \hat{z}_{i,m+1}, \hat{\beta}_i, y_{i,ref} \dots y_{i,ref}^{(m+1)})\} \\ & + \sum_{k=1}^{p} 2^{2k}\{d_{ik} + \upsilon_{ik} + (m+1)(d_{1ik} + \upsilon_{1ik})\}\{\|\chi_{i1}\|^{2k} + \|y_{i,ref}\|^{2k}\} \\ & +\sigma_i\beta_i^{*2} - 2\beta_i^*\varrho_i \sum_{k=1}^{p} k\chi_{i1}^{2k}\Bigg]. \end{aligned} \tag{1.33}$$

With $\hat{z}_{i,m+2}$ as the *virtual* control for the $(\chi_{i1} \dots \chi_{i,m+1})$ subsystem, we choose

$$\begin{aligned}\hat{z}_{i,m+2} &= -\Big[\pi_{i,m+1}\chi_{i,m+1} + \chi_{im} + \varsigma_{i,m+1}(y_i, \hat{z}_{i1} \dots \hat{z}_{i,m+1}, \hat{\beta}_i, y_{i,ref} \dots y_{i,ref}^{(m+1)}) \\ &\quad +\chi_{i,m+1}\varpi_{i,m+1}^2(y_i, \hat{z}_{i1} \dots \hat{z}_{i,m+1}, \hat{\beta}_i, y_{i,ref} \dots y_{i,ref}^{(m+1)})\Big] \\ &\triangleq \tau_{i,m+1}(y_i, \hat{z}_{i1} \dots \hat{z}_{i,m+1}, \hat{\beta}_i, y_{i,ref} \dots y_{i,ref}^{(m+1)}) \end{aligned} \tag{1.34}$$

with $\pi_{i,m+1} > 0$. Define: $\chi_{i,m+2} = \hat{z}_{i,m+2} - \tau_{i,m+1}(y_i, \hat{z}_{i1} \dots \hat{z}_{i,m+1}, \hat{\beta}_i, y_{i,ref} \dots y_{i,ref}^{(m+1)})$. Then, $\dot{V}_m$ is given by

$$\begin{aligned}\dot{V}_m \leq \sum_{i=1}^{N} \Bigg[& -\{\lambda_{min}(Q_i) - (m+3)\}\|\epsilon_i\|^2 - \sigma_i(\hat{\beta}_i - \beta_i^*)^2 - 2\pi_{i1}\varrho_i \sum_{k=1}^{p} \chi_{i1}^{2k} - 2\sum_{j=2}^{m+1} \pi_{ij}\chi_{ij}^2 \\ & +2\chi_{i,m+1}\chi_{i,m+2} + \sum_{k=1}^{p} 2^{2k}\{d_{ik} + \upsilon_{ik} + (m+1)(d_{1ik} + \upsilon_{1ik})\}\{\|\chi_{i1}\|^{2k} + \|y_{i,ref}\|^{2k}\} \end{aligned}$$

$$+\sigma_i\beta_i^{*2} - 2\beta_i^*\varrho_i\sum_{k=1}^{p} k\chi_{i1}^{2k}\Bigg]. \tag{1.35}$$

Step $\rho-1$: In step $\rho-2$, $\hat{z}_{i,\rho}$ was derived as the virtual control input $(=\tau_{i,\rho-1}(y_i,\hat{z}_{i1}\ldots\hat{z}_{i,\rho-1},\hat{\beta}_i,y_{i,ref}\ldots y_{i,ref}^{(\rho-1)}))$ for the $(\chi_{i1}\ldots\chi_{i,\rho-1})$ subsystem. Define

$$\chi_{i,\rho} = \hat{z}_{i,\rho} - \tau_{i,\rho-1}(y_i,\hat{z}_{i1}\ldots\hat{z}_{i,\rho-1},\hat{\beta}_i,y_{i,ref}\ldots y_{i,ref}^{(\rho-1)}).$$

The *actual* control input u_i now appears in the state equation for $\chi_{i,\rho}$, i.e.,

$$\begin{aligned}\dot{\chi}_{i,\rho} &= b_{i,\kappa_i-\rho}\delta_i(y_i)u_i + \hat{z}_{i,\rho+1} + \varsigma_{i,\rho}(y_i,\hat{z}_{i1}\ldots\hat{z}_{i,\rho},\hat{\beta}_i,y_{i,ref}\ldots y_{i,ref}^{(\rho)})\\ &\quad+\varpi_{i,\rho}(y_i,\hat{z}_{i1}\ldots\hat{z}_{i,\rho},\hat{\beta}_i,y_{i,ref}\ldots y_{i,ref}^{(\rho)})\{\epsilon_{i2}+\varphi_{i1}(y_1\ldots y_N)+\xi_{i1}(y_1\ldots y_N)\omega(t)\}\end{aligned} \tag{1.36}$$

The composite Lyapunov function for the overall system is given by: $V_{\rho-1} = V_{\rho-2} + \sum_{i=1}^{N}\chi_{i,\rho}^2$.
Differentiating $V_{\rho-1}$ along the trajectories of the $(\chi_{i1}\ldots\chi_{i,\rho})$ subsystem and following steps similar to (1.30)-(1.32), we obtain

$$\begin{aligned}\dot{V}_{\rho-1} \;\le\; \sum_{i=1}^{N}\Bigg[&-\{\lambda_{min}(Q_i)-(\rho+2)\}\|\epsilon_i\|^2 - \sigma_i(\hat{\beta}_i-\beta_i^*)^2 - 2\pi_{i1}\varrho_i\sum_{k=1}^{p}\chi_{i1}^{2k} - 2\sum_{j=2}^{\rho-1}\pi_{ij}\chi_{ij}^2\\ &+2\chi_{i,\rho}\{b_{i,\kappa_i-\rho}\delta_i(y_i)u_i + \hat{z}_{i,\rho+1} + \chi_{i,\rho-1} + \varsigma_{i,\rho}(y_i,\hat{z}_{i1}\ldots\hat{z}_{i,\rho},\hat{\beta}_i,y_{i,ref}\ldots y_{i,ref}^{(\rho)})\\ &+\chi_{i,\rho}\varpi_{i,\rho}^2(y_i,\hat{z}_{i1}\ldots\hat{z}_{i,\rho},\hat{\beta}_i,y_{i,ref}\ldots y_{i,ref}^{(\rho)})\} + \sigma_i\beta_i^{*2}\\ &+\sum_{k=1}^{p}2^{2k}\{d_{ik}+\upsilon_{ik}+\rho(d_{1ik}+\upsilon_{1ik})\}\{\|\chi_{i1}\|^{2k}+\|y_{i,ref}\|^{2k}\} - 2\beta_i^*\varrho_i\sum_{k=1}^{p}k\chi_{i1}^{2k}\Bigg]\end{aligned} \tag{1.37}$$

The following decentralized control input u_i is now applied for the ith subsystem

$$\begin{aligned}u_i \;=\; &-\frac{1}{b_{i,\kappa_i-\rho}\delta_i(y_i)}\Big\{\pi_{i,\rho}\chi_{i,\rho} + \hat{z}_{i,\rho+1} + \chi_{i,\rho-1} + \varsigma_{i,\rho}(y_i,\hat{z}_{i1}\ldots\hat{z}_{i,\rho},\hat{\beta}_i,y_{i,ref}\ldots y_{i,ref}^{(\rho)})\\ &+\chi_{i,\rho}\varpi_{i,\rho}^2(y_i,\hat{z}_{i1}\ldots\hat{z}_{i,\rho},\hat{\beta}_i,y_{i,ref}\ldots y_{i,ref}^{(\rho)})\Big\}.\end{aligned} \tag{1.38}$$

The properties of the above designed decentralized control law are stated in the following theorem.

Theorem 1.3.1 Suppose that the system (1.1) is transformable to the observer canonical form (1.2) and satisfies assumptions (2.2) – (2.4). The decentralized control (1.38) along with adaptation law (1.12) for $\hat{\beta}_i$ results in global uniform boundedness of all the signals of the closed-loop system comprised of the plant (1.1) with disturbance $\omega(t)$, the observer (1.5), the adaptation gain $\hat{\beta}_i$ and the control input u_i $(1\le i\le N)$. Furthermore, the disturbance signal does not affect the tracking error $(y_i - y_{i,ref})$ and the error can be made arbitarily small based on appropriate choice of the control

gains π_{ij}. For the regulation problem, global regulation of the states of the plant and observer is achieved.

Proof of Theorem 1.3.1: With the control (1.38), we first show the existence of β_i^* to counter the effects of the interconnections. One such choice is given by

$$\beta_i^* \geq \frac{1}{\varrho_i} \max_{k=1\ldots p} \{d_{ik} + \upsilon_{ik} + \rho(d_{1ik} + \upsilon_{1ik})\}.$$

With $\lambda_{min}(Q_i) = 2\pi_{i0} + \rho + 2$, $\pi_{i0} > 0$, we obtain

$$\begin{aligned}
\dot{V}_{\rho-1}(\epsilon, \chi_1 \ldots \chi_\rho, \hat{\beta}) \leq \sum_{i=1}^{N} \Bigg[& -2\pi_{i0}\|\epsilon_i\|^2 - 2\pi_{i1}\varrho_i \sum_{k=1}^{p} \chi_{i1}^{2k} - 2\sum_{j=2}^{\rho} \pi_{ij}\chi_{ij}^2 - \sigma_i(\hat{\beta}_i - \beta_i^*)^2 \\
& + \sigma_i\beta_i^{*2} + \sum_{k=1}^{p} 2^{2k}\{d_{ik} + \upsilon_{ik} + \rho(d_{1ik} + \upsilon_{1ik})\}\|y_{i,ref}\|^{2k} \Bigg] \\
\leq \; & -\mu V_{\rho-1}(\epsilon, \chi_1 \ldots \chi_\rho, \hat{\beta}) + \psi \qquad (1.39)
\end{aligned}$$

where $\chi_j = [\chi_{1j} \ldots \chi_{Nj}]$, $\hat{\beta} = [\hat{\beta}_1 \ldots \hat{\beta}_N]$ and

$$\mu = \min_{1\leq i\leq N} \left(\min\{2\pi_{i0}\lambda_{max}^{-1}(P_i), 2\pi_{i1} \ldots 2\pi_{i\rho}, \Gamma_i\sigma_i\}\right) \qquad (1.40)$$

$$\psi = \sum_{i=1}^{N} \left\{ \sigma_i\beta_i^{*2} + \sum_{k=1}^{p} 2^{2k}\{d_{ik} + \upsilon_{ik} + \rho(d_{1ik} + \upsilon_{1ik})\}\|y_{i,ref}\|^{2k} \right\}. \qquad (1.41)$$

ψ is bounded since β^* and y_{ref} are bounded. Thus, $V_{\rho-1}(\epsilon, \chi_1 \ldots \chi_\rho, \hat{\beta})$ decreases monotonically along the solutions of the $(\epsilon, \chi_1 \ldots \chi_\rho, \hat{\beta})$ dynamics until it reaches the compact set

$$\Omega_f = \left\{ (\epsilon, \chi_1 \ldots \chi_\rho, \hat{\beta}) \in \mathcal{R}^{\sum_{j=1}^{N}\kappa_j} \times \mathcal{R}^N \times \ldots \times \mathcal{R}^N \times \mathcal{R}^N : V_{\rho-1}(\epsilon, \chi_1 \ldots \chi_\rho, \hat{\beta}) \leq V_f \right\} \qquad (1.42)$$

where $V_f = \mu^{-1}\psi$. Thus, the solutions $(\epsilon, \chi_1 \ldots \chi_\rho, \hat{\beta})$ are globally ultimately bounded with respect to the bound V_f. The boundedness of other signals is established as follows. Boundedness of $z_{i1}(= y_i)$ and $\tau_{i1}(\chi_{i1}, \hat{\beta}_i)$ follows from that of χ_{i1}, $\hat{\beta}_i$ and $y_{i,ref}$. Since χ_{i2} is bounded, from (1.11) we have bounded $\hat{z}_{i2}$. Iteratively, from boundedness of y_i, $\hat{z}_{i1} \ldots \hat{z}_{im}$, $y_{i,ref} \ldots y_{i,ref}^{(m)}$, $\hat{\beta}_i$, $\chi_{i,m+1}$, and from (1.26), boundedness of $\hat{z}_{i,m+1}$ is established $\forall\ 1 \leq i \leq N$, $\forall\ 1 \leq m \leq \rho - 1$. Since ϵ_i are bounded, we obtain bounded $z_{i1} \ldots z_{i\rho}$.

To prove boundedness of $z_{i,\rho+1} \ldots z_{i,\kappa_i}$, we use the transformation, $\eta_i = Tz_i$, with $(\eta_{i1} \ldots \eta_{i\rho}) = (z_{i1} \ldots z_{i\rho})$ and

$$\eta_{ij} \;=\; z_{ij} - \frac{b_{i,\kappa_i-j}}{b_{i,\kappa_i-\rho}} z_{i\rho}, \;\; j = \rho - 1 \ldots \kappa_i \qquad (1.43)$$

to obtain

$$\begin{aligned}
\dot{\eta}_{ij} &= \eta_{i,j+1} + \varphi_{ij}(y_1 \dots y_N), \quad j = 1 \dots \rho - 1 \\
\dot{\eta}_{i\rho} &= \eta_{i,\rho+1} + \frac{b_{i,\kappa_i-\rho_i-1}}{b_{i,\kappa_i-\rho_i}}\eta_{i,\rho} + \varphi_{i,\rho}(y_1 \dots y_N) + b_{i,\kappa_i-\rho}\delta_i(y_i)u_i \\
\dot{\eta}_{ij} &= -\frac{b_{i,\kappa_i-j}}{b_{i,\kappa_i-\rho}}\eta_{i,\rho+1} + \eta_{i\rho}\left\{\frac{b_{i,\kappa_i-j-1}}{b_{i,\kappa_i-\rho}} - \frac{b_{i,\kappa_i-j}b_{i,\kappa_i-\rho-1}}{b_{i,\kappa_i-\rho}^2}\right\} \\
&\quad + \left\{\varphi_{i,\rho+1}(y_1 \dots y_N) - \frac{b_{i,\kappa_i-j}}{b_{i,\kappa_i-\rho}}\varphi_{i,\rho}(y_1 \dots y_N)\right\}, \quad j = \rho+1 \dots \kappa_i - 1 \\
\dot{\eta}_{i,\kappa_i} &= -\frac{b_{i0}}{b_{i,\kappa_i-\rho}}\eta_{i,\rho+1} - \eta_{i\rho}\frac{b_{i0}b_{i,\kappa_i-\rho-1}}{b_{i,\kappa_i-\rho}^2} + \left\{\varphi_{i,\kappa_i}(y_1 \dots y_N) - \frac{b_{i,0}}{b_{i,\kappa_i-\rho}}\varphi_{i,\rho}(y_1 \dots y_N)\right\} \quad (1.44)
\end{aligned}$$

The boundedness of $(\eta_{i,\rho+1} \dots \eta_{i,\kappa_i})$ now follows from (1.44) since $\eta_{i,\rho} = z_{i\rho}$ and $(y_1 \dots y_N)$ (and hence $\varphi_{ij}(y_1 \dots y_N)$) are bounded, and the zero dynamics are exponentially stable (Assumption (2.2)). Thus $z_i = T^{-1}\eta_i$ are bounded $\forall\ 1 \leq i \leq N$. Boundedness of u_i now follows from (1.38) since $\hat{z}_{i,\rho+1}$ is bounded and $b_{i,\kappa_i-\rho}\delta_i(y_i)$ is bounded away from zero. Boundedness of the states x of the original system (1.1) follows since $z = \Phi(x)$ is a global diffeomorphism.

The size of residual set Ω_f given by (1.42), and hence the tracking error can be made arbitrarily small by increasing the magnitude of the control gains π_{ij}. Note that, from definitions of μ and ψ, we have $\psi \propto \sigma_i$, $\mu \propto \sigma_i$ and $\mu \propto \Gamma_i$. Choosing $\Gamma_i \propto \frac{1}{\sigma_i^2}$, as $\sigma_i \to 0$, $\psi \to 2\sum_{k=1}^{p} k(d_{ik} + \rho d_{1ik})\|y_{i,ref}\|^{2k}$. Also, from (1.40), $\Gamma_i\sigma_i$ will increase and the value of μ will be determined by the control gains π_{ij}, $1 \leq j \leq \rho$. Thus, reducing σ_i and increasing π_{ij} will reduce the the size of the residual error bound $V_f = \mu^{-1}\psi$.

Regulation: For the regulation problem, $y_{i,ref} \equiv 0$. In this case, we set σ_i in the adaptation law (1.12) to zero. Thus, $\psi = 0$. Following the same procedure as in the tracking case, $\dot{V}_{\rho-1}$ is given by

$$\dot{V}_{\rho-1}(\epsilon, \chi_1 \dots \chi_\rho, \hat{\beta}) \leq \sum_{i=1}^{N}\left[-2\pi_{i0}\|\epsilon_i\|^2 - 2\pi_{i1}\varrho_i\sum_{k=1}^{p}\chi_{i1}^{2k} - 2\sum_{j=2}^{\rho}\pi_{ij}\chi_{ij}^2\right], \quad (1.45)$$

which implies that the solutions $\epsilon, \chi_1 \dots \chi_\rho, \hat{\beta}$ are bounded for all initial conditions and for all t. A straightforward application of LaSalle's theorem yields

$$\lim_{t\to\infty}\epsilon_i(t) = 0, \qquad \lim_{t\to\infty}\chi_{ij}(t) = 0; \qquad 1 \leq j \leq \rho; 1 \leq i \leq N,$$

i.e., the tracking error $\chi_{i1} = y_i - y_{i,ref}$ and the observer error ϵ_i go to zero asymptotically. □

Remark 3.2: In contrast to [11], where p parameters need to be adapted corresponding to $\sum_{j=1}^{p}\theta_j\varphi_j(y)$, the adaptive scheme proposed here requires adaptation of

only one parameter $\hat{\beta}_i$. This is true even if the interconnections in (1.2) were given by $\sum_{j=1}^{p} \theta_j \varphi_{ij}(y_1 \dots y_N)$ as long as φ_{ij} satisfies assumption (1.3). The trade-off, however, is loss of asymptotic tracking and utilization of high control gains as in [12] to counter the uncertainties.

Remark 3.3: Even in the absence of the disturbance $\omega(t)$, the tracking error would be bounded, but nonzero, with a smaller size of the residual set Ω_f in (1.42) since $v_{1ik} = v_{ik} = 0$ in this case. The tracking error due to disturbance is proportional to ω_{max}; however, the components (frequencies) of the disturbance signal are asymptotically rejected in the output. With appropriate choice of control gains, this error can be made arbitrarily small.

Remark 3.4: An important issue in control of large scale systems is to ensure that the existing decentralized controllers maintain stability and robust performance, if subsystems are appended to the original system, or taken off-line, e.g., during faults in a power system. The design methodology proposed here obviates the need for controller redesign as long as the order of the interconnections due to the appended subsystem is less than or equal to that of the original system. This is generally true for most practical applications where the interconnected subsystems are dynamically similar. In any case, defining p as the maximum *possible* order of all current and future interconnections will ensure that the same decentralized controller works for the modified system.

Remark 3.5: From the above design procedure, it is clear that after the 0th step, the virtual controls can be assigned independently to each subsystem. Therefore, even the case where the relative degrees of the subsystems are different, can be treated similarly.

1.4 Conclusion

In this report, we have extended the class of large scale nonlinear systems for which decentralized output feedback controllers can be designed. The distinguishing features of this report which makes it different from all previously reported decentralized output feedback schemes are the relaxation of bounds on the interconnections from linear to higher order bounds, the mismatch between the interconnections and the control, and the ability to reject any bounded, unmeasurable disturbance entering the system. The stability and robustness properties attained are global. Although, the scheme does not guarantee asymptotic tracking, the bounds on the tracking error can be made arbitrarily small through proper choice of control gains. For the case, where the objective is regulation, global asymptotic regulation of all the states of the closed-loop system is achieved. One potential application of the proposed scheme is in robust decentralized design for large-scale power systems with swing angle measurements only which is discussed in [14].

1.5 References

[1] A. Datta and P. Ioannou, "Decentralized indirect adaptive control of interconnected systems," *International Journal of Adaptive Control and Signal Processing*, vol. 5, no. 4, pp. 259–281, 1991.

[2] R. Ortega and A. Herrera, "A solution to the decentralized adaptive stabilization problem," *Systems & Control Letters*, vol. 20, pp. 299–306, 1993.

[3] C. Wen, "Decentralized adaptive regulation," *IEEE Transactions on Automatic Control*, vol. AC-39, pp. 2163–2166, Oct. 1994.

[4] C. Wen, "Indirect robust totally decentralized adaptive control of continuous time interconnected systems," *IEEE Transactions on Automatic Control*, vol. AC-40, pp. 1122–1126, June 1995.

[5] Ö. Hüseyin, M. E. Sezer, and D. D. Šiljak, "Robust decentralized control using output feedback," *IEE Proceedings*, vol. 129-D, no. 6, pp. 310–314, 1982.

[6] P. A. Ioannou, "Decentralized adaptive control of interconnected systems," *IEEE Transactions on Automatic Control*, vol. AC–31, pp. 291–298, Apr. 1986.

[7] D. T. Gavel and D. D. Šiljak, "Decentralized adaptive control: structural conditions for stability," *IEEE Transactions on Automatic Control*, vol. AC-34, no. 4, pp. 413–426, 1989.

[8] L. Shi and S. K. Singh, "Decentralized control for interconnected uncertain systems: extensions to higher-order uncertainties," *Int. Journal of Control*, vol. 57, no. 6, pp. 1453–1468, 1993.

[9] S. Jain and F. Khorrami, "Global decentralized adaptive control of large scale nonlinear systems without strict matching," in *Proceedings of the 1995 American Control Conference*, (Seattle, WA), pp. 2938–2942, June 1995.

[10] I. Kanellakopoulos, P. V. Kokotović, and A. S. Morse, "A toolkit for nonlinear feedback design," *Systems & Control Letters*, vol. 19, pp. 177–185, 1992.

[11] I. Kanellakopoulos, M. Krstić, and P. V. Kokotović, "κ-adaptive control of output-feedback nonlinear systems," in *Proceedings of the 32nd Conference on Decision and Control*, (San Antonio, TX), pp. 1061–1066, Dec. 1993.

[12] R. Marino and P. Tomei, "Global adaptive output feedback control of nonlinear systems, part II: nonlinear parameterization," *IEEE Transactions on Automatic Control*, vol. AC-38, no. 1, pp. 33–48, 1993.

[13] S. Jain and F. Khorrami, "Decentralized adaptive output feedback control of large scale interconnected nonlinear systems," in *Proceedings of the 1995 American Control Conference*, (Seattle, WA), pp. 1600–1604, June 1995.

[14] S. Jain and F. Khorrami, "Application of a decentralized adaptive output feedback based on backstepping to power systems," in *Proceedings of the 34th Conference on Decision and Control*, (New Orleans, LA), pp. 1585–1590, Dec. 1995.

2. Parametrization of Stable Systems from Partial Impulse Response Sequences

2.1 Introduction

This report addresses the problem of identifying the class of all stable system transfer functions that interpolate the given partial impulse response sequence. Although classical Padé approximations match the given impulse response sequence to a maximum extent and are optimal in that sense, the systems so obtained need not be stable and hence they may not be attractive from physical considerations. In this context, consider the problem of identifying a linear discrete time-invariant, causal, stable system with an unknown transfer function $H(z)$ from partial information regarding itself. Since the system is causal, it has a one-sided power series expansion given by

$$H(z) = \sum_{k=0}^{\infty} h_k z^k \tag{2.1}$$

and stability demands that

$$\sum_{k=0}^{\infty} |h_k| < \infty . \tag{2.2}$$

It follows from (2.1), (2.2) and uniform convergence that the transfer function $H(z)$ is analytic in $|z| < 1$ and uniformly continuous[1] in $|z| \leq 1$ [1,2]. Clearly, the sequence $\{h_k\}_{k=0}^{\infty}$ represents the impulse response of the system and when the available information is of the form h_k, $k = 0 \rightarrow n$, the system identification problem in the rational case becomes equivalent to a Padé approximation problem. In that case, it is easy to show that rational ARMA(p, q)-type approximations that match the given data are unique provided $p + q \leq n$ (Padé approximation) [1,2]. These approximations, however, need not be stable and hence from physical considerations they may not be acceptable. For example, consider the stable (minimum phase) transfer function $H(z) = e^{-3z}$. The ARMA(1,1) Padé approximation of this function is given by $(2 - 3z)/(2 + 3z)$, and it represents an unstable system since $A_1(z)$ has a zero in $|z| < 1$.

In the rational case the identification problem is equivalent to finding the system model order (p, q) and the system parameters. Given the partial impulse response sequence, the system model can be established from the invariance of the rank property

[1]Note that the use of the variable z (rather than z^{-1}) here translates all stability arguments into the compact region $|z| \leq 1$. $H(z)$ is said to be minimum phase if it is analytic together with its inverse in $|z| < 1$. Since stable functions are free of poles in $|z| \leq 1$, in the rational case they are analytic in $|z| \leq 1$.

associated with certain Hankel matrices generated from this data. Thus, in particular, with h_k, $k \geq 0$, denoting its impulse response sequence as in (2.1), let

$$H_k \triangleq \begin{bmatrix} h_1 & h_2 & \cdots & h_k \\ h_2 & h_3 & \cdots & h_{k+1} \\ \vdots & \vdots & \vdots & \vdots \\ h_k & h_{k+1} & \cdots & h_{2k-1} \end{bmatrix} \tag{2.3}$$

represent the Hankel matrix of size $k \times k$ generated from h_1, h_2, $\cdots h_{2k-1}$. Then, for a rational system with degree p,

$$\text{rank}\, H_k = \text{rank}\, H_p = p\,, \quad k \geq p \tag{2.4}$$

and several singular value decomposition technique have been proposed for model order selection based on the above rank condition [3,4]. Equation (2.4) shows the linear dependence of h_{p+1}, h_{p+2}, $\cdots$ on their p previous terms, and it represents the finite degree nature of a rational system. Although these techniques have the advantage that they can make use of all available impulse response data, they need not lead to stable systems. Moreover, the above rank condition is not valid in the case of systems that are not rational, since they do not represent finite degree systems. The problem in that case is to obtain equivalent finite degree stable rational approximations that capture all the key features of the original nonrational system in an optimal manner by making use of the given data. Such a rational approximation should interpolate the given information, and preferably be of minimum possible degree.

In this report, we address this problem and obtain closed form solutions for the class of all stable transfer functions that interpolate the given partial impulse response sequence. Specifically, by making contact with the Schur problem [5] in, it is shown in section II that the theory of bounded functions (Schur functions) can be utilized to obtain all stable solutions to this problem. In this context, a new model order selection procedure is proposed here that utilizes the finite degree property of a rational system. Rational and stable approximation of nonrational systems is described in section III, by making use of ideas developed in section II. Although various authors have addressed related problems in the past utilizing this approach [6]-[14], some interesting new observations will show that rational system identification as well as stable rational approximation of nonrational functions can be realized from the same formulation of the Schur extension problem.

2.2 Parametrization of Stable Systems

2.2.1 The Schur Parametrization

To start with, a function $d(z)$ is said to be bounded (Schur function), if (i) $d(z)$ is analytic in $|z| < 1$ and (ii) $|d(z)| \leq 1$, in $|z| < 1$. Because of the analyticity in $|z| < 1$, every bounded function possesses a power series representation of the form

$d(z) = \sum_{k=0}^{\infty} d_k z^k$, $|z| < 1$, that is valid in $|z| < 1$. If $d(z)$ is rational, then $|d(z)| \leq 1$ in $|z| < 1$ also implies $d(z)$ is free of poles in $|z| = 1$ and hence $d(z)$ is analytic in $|z| \leq 1$. As a result $d(z)$ represents a stable system.

¿From Schur's Theorem [5], $d(z)$ defined above represents a bounded function iff

$$\mathbf{I} - \mathbf{D}_k \mathbf{D}_k^* \geq 0\,, \quad k = 0 \rightarrow \infty\,, \tag{2.5}$$

where

$$\mathbf{D}_k \triangleq \begin{pmatrix} d_0 & 0 & 0 & \cdots & 0 \\ d_1 & d_0 & 0 & \cdots & 0 \\ d_2 & d_1 & d_0 & \cdots & 0 \\ \vdots & \vdots & \vdots & \ddots & \vdots \\ d_k & d_{k-1} & d_{k-2} & \cdots & d_0 \end{pmatrix} \tag{2.6}$$

represents the lower (or upper) triangular Toeplitz matrix generated from d_i, $i = 0 \rightarrow k$.

Given a partial set of coefficients d_k, $k = 0 \rightarrow n$, that satisfy $\mathbf{I} - \mathbf{D}_n \mathbf{D}_n^* \geq 0$, "the problem of coefficients" is to obtain all bounded functions $d(z)$ such that the power series expansion of $d(z)$ matches the given coefficients, i.e., $d(z) = \sum_{k=0}^{n} d_k z^k + O(z^{n+1})$.

An algorithm introduced by Schur in this context answers this problem and it forms the basis for our approach to the present parametrization problem. As Schur has first observed, if $d(z)$ represents a bounded function, then, so does the function[5]

$$d_1(z) \triangleq \frac{1}{z} \cdot \frac{d(z) - d(0)}{1 - d^*(0) d(z)}\,, \quad d(0) = d_0\,. \tag{2.7}$$

In the rational case, since $z = 0$ is not a pole of $d_1(z)$, from (2.7) we obtain that the degree[2] of the new bounded function $d_1(z)$ never exceeds that of $d(z)$, i.e.,

$$\delta(d_1(z)) \leq \delta(d(z))\,, \tag{2.8}$$

with inequality iff the $1/z$ factor in (2.7) cancels a pole of $(d(z) - d_0)/(1 - d_0^* d(z))$ [17]. Since this cancellation can occur only at $z = \infty$, from (2.7)–(2.8), degree reduction happens iff the denominator term $1 - d(0)^* d(z)$ satisfies $1 - d^*(0) d(z)|_{z=\infty} = 0$, or

$$\delta(d_1(z)) < \delta(d(z)) \;\Leftrightarrow\; d(z) d_*(z)|_{z=0} = 1\,, \tag{2.9}$$

where

$$d_*(z) \triangleq d^*(1/z^*) \tag{2.10}$$

[2]The degree $\delta(H(z))$ of a rational function $H(z)$ equals the totality of its poles (or zeros), with multiplicities counted, including those at infinity.

is defined to be the paraconjugate form of $d(z)$. Clearly, the paraconjugate form represents the ordinary complex conjugate operation on the unit circle.

The bilinear transformation in (2.7) maps the inside of the unit circle onto itself. Thus, in general, with $d_k(z)$ representing an arbitrary bounded function and with

$$s_k \triangleq d_k(0)\,, \tag{2.11}$$

(2.7) translates into

$$d_{k+1}(z) = \frac{1}{z} \cdot \frac{d_k(z) - s_k}{1 - s_k^* d_k(z)}\,, \quad k \geq 0 \tag{2.12}$$

with the understanding that $d_0(z) \equiv d(z)$. The above Schur algorithm can be recursively updated and after n such steps, we get

$$d(z) = \frac{b_n(z) + z\tilde{a}_n(z) d_{n+1}(z)}{a_n(z) + z\tilde{b}_n(z) d_{n+1}(z)}\,, \tag{2.13}$$

where $a_n(z)$ and $b_n(z)$ are in general two polynomials of degree n, and

$$\tilde{a}_n(z) \triangleq z^n a_{n*}(z) = z^n a_n^*(1/z^*)\,, \tag{2.14}$$

$$\tilde{b}_n(z) \triangleq z^n b_{n*}(z) = z^n b_n^*(1/z^*) \tag{2.15}$$

represent polynomials reciprocal to $a_n(z)$ and $b_n(z)$ respectively that satisfy the recursion

$$a_n(z) \triangleq a_{n-1}(z) + z s_n \tilde{b}_{n-1}(z)\,, \quad n \geq 1 \tag{2.16}$$

and

$$b_n(z) \triangleq b_{n-1}(z) + z s_n \tilde{a}_{n-1}(z)\,, \quad n \geq 1. \tag{2.17}$$

$a_n(z)$ and $b_n(z)$ are defined to be the Schur polynomials of the first and second kind respectively. Notice that, if $d(z)$ is rational to start with, application of the above procedure will result in a rational bounded function $d_{n+1}(z)$ for every n, and, further from (2.8), in that case $\delta(d_{n+1}(z)) \leq \delta(d(z))\,, \quad n \geq 0$. ¿From (2.13), the iterations in (2.16)–(2.17) start with

$$a_0(z) = 1\,, \quad b_0(z) = s_0 = d_0\,. \tag{2.18}$$

Using (2.16)–(2.17), it is easy to show that $a_n(z)\,,\ n = 1 \rightarrow \infty$, represent strict Hurwitz polynomials[3]. In particular with $d_{n+1}(z) \equiv 0$, we have $d(z) = b_n(z)/a_n(z)$

[3]A Hurwitz polynomial is free of zeros in $|z| < 1$, and a strict Hurwitz polynomial is free of zeros in $|z| \leq 1$.

itself is bounded and, moreover, a direct expansion gives $d(z) - \frac{b_n(z)}{a_n(z)} = O(z^{n+1})$; i.e., the power series expansions of the bounded functions $d(z)$ and $b_n(z)/a_n(z)$ agree upto the first $n+1$ terms and hence the above terms *must* be independent of $d_{n+1}(z)$. Thus, for every arbitrary bounded function $d_{n+1}(z)$, we must have the interpolation property

$$d(z) = \frac{b_n(z) + z\tilde{a}_n(z)d_{n+1}(z)}{a_n(z) + z\tilde{b}_n(z)d_{n+1}(z)} = \sum_{k=0}^{n} d_k z^k + O(z^{n+1}), \tag{2.19}$$

and the d_k's, $k = 0 \rightarrow n$, can be determined from the Schur polynomials $a_k(z)$, $b_k(z)$ in (2.16)–(2.18). Conversely, (2.19) is completely specified by the first $(n+1)$ coefficients $\{d_k\}_{k=0}^{n}$, or, from the Schur polynomials $a_n(z)$ and $b_n(z)$. To complete the recursions in (2.16)–(2.18), only the coefficients s_k, $k = 0 \rightarrow n$, are required and they can be obtained recursively from the given data d_k, $k = 0 \rightarrow n$ as

$$s_0 = d_0 \tag{2.20}$$

and

$$s_n = \frac{\sum_{k=0}^{n-1} a_k^{(n-1)} d_{n-k}}{1 - \sum_{k=0}^{n-1} b_k^{(n-1)^*} d_k} = \frac{\left\{ a_{n-1}(z) \sum_{k=1}^{n} d_k z^k \right\}_n}{1 - \left\{ \tilde{b}_{n-1}(z) \sum_{k=0}^{n-1} d_k z^k \right\}_{n-1}}, \quad n \geq 1. \tag{2.21}$$

where $\{\ \}_n$ represents the coefficient of z^n in $\{\ \}$. Using this, $a_n(z)$ and $b_n(z)$ can be computed recursively, and the class of all bounded functions that interporate the given coefficients d_k, $k = 0 \rightarrow n$ is given by $d(z)$ in (2.19).

In general, the given impulse response data h_k, $k = 0 \rightarrow n$, do not form part of a bounded function, and to make use of the above formulation in section II, it is necessary to 'prepare' this data so that it confirms with a bounded function. To attain this goal, consider the matrix

$$\mathbf{H}_n = \begin{pmatrix} h_0 & 0 & \cdots & 0 \\ h_1 & h_0 & \cdots & 0 \\ \vdots & \vdots & \ddots & \vdots \\ h_n & h_{n-1} & \cdots & h_0 \end{pmatrix}, \tag{2.22}$$

and let $\lambda_1^2(n)$ represent the largest eigenvalue of $\mathbf{H}_n\mathbf{H}_n^*$. Then, clearly, the sequence

$$d_k \triangleq \frac{h_k}{\kappa_n}, \quad \kappa_n > \lambda_1(n), \quad k = 0 \rightarrow n, \tag{2.23}$$

satisfies (2.5) with inequality, and hence qualifies as the first $n+1$ coefficients of a bounded function. Recursive determination of the coefficients s_k, $k = 0 \rightarrow n$ from (2.20)–(2.21), together with $a_k(z)$ and $b_k(z)$, $k = 0 \rightarrow n$ using (2.16)–(2.18), gives

$$H(z) = \kappa_n \cdot \frac{b_n(z) + z\tilde{a}_n(z)d_{n+1}(z)}{a_n(z) + z\tilde{b}_n(z)d_{n+1}(z)} = \sum_{k=0}^{n} h_k z^k + O(z^{n+1}) \tag{2.24}$$

to be the class of all transfer functions that are analytic in $|z| < 1$, free of poles in $|z| \leq 1$ and interpolate the given partial impulse response sequence h_k, $k = 0 \rightarrow n$.

Equation (2.24) can be given two interesting interpretations: First, if a system transfer function $H(z)$ is rational to start with, then its representation as in (2.24) after n steps of the Schur algorithm will imply that $d_{n+1}(z)$ must be a rational function. Similiarly if $H(z)$ is nonrational to start with, then $d_{n+1}(z)$ must be nonrational in (2.24).

The alternate interpretation shows that given h_0, h_1, $\cdots h_n$, equation (2.24) represents all stable system transfer functions both rational and nonrational that interpolate the given data, and they can be obtained by varying $d_{n+1}(z)$ over all bounded functions. Thus even if the given data corresponds to a nonrational system, the freedom present in the choice of $d_{n+1}(z)$ in (2.24) can be utilized for rational approximation of $H(z)$ by appropriate choice of rational bounded functions $d_{n+1}(z)$.

The above discussion shows that $d_{n+1}(z)$ can be utilized for rational system identification as well as rational approximation of nonrational systems. In particular, if $d_{n+1}(z)$ is chosen to be a rational bounded function, then since $d_{n+1}(z)$ and $H(z)$ are free of poles in $|z| \leq 1$, $H(z)$ in (2.24) represents a stable regular rational transfer function (analytic in $|z| \leq 1$) that matches the given coefficients. As a result, the class of all stable rational functions that interpolate the given impulse response sequence is obtained from (2.24) by varying $d_{n+1}(z)$ over all rational bounded functions.

2.2.2 The Rational Case

If $d(z)$ in (2.13) is rational to start with, repeated application of the Schur procedure will result in rational bounded functions $d_{n+1}(z)$ that satisfy the degree constraint in (2.8)–(2.9). As a result, from (2.19) and (2.24), it follows that every stable rational function $H(z)$ can be represented as in (2.24) where $d_{n+1}(z)$ is a unique rational bounded function that satisfies

$$\delta(d_{n+1}(z)) \leq \delta(H(z)), \tag{2.25}$$

and degree reduction in (2.25) happens according to (2.9). Thus if $H(z)$ represents a stable ARMA(p,q) system with $p > q$ in (2.24), then $\delta(H(z)) = p$ and since $\frac{b_0 b_p^*}{a_0 a_p^*} = 0$, it follows from that

$$\delta(d_{n+1}(z)) = p \tag{2.26}$$

and further using the degree arguments as in (2.8), we obtain

$$d_{n+1}(z) = \frac{f(z)}{g(z)} = \frac{f_0 + f_1 z + \cdots + f_{p-1} z^{p-1}}{1 + g_1 z + g_2 z + \cdots + g_p z^p}, \quad n \geq 1. \tag{2.27}$$

(Since $g(z)$ is strict Hurwitz, $g_0 \neq 0$ and it is normalized here to unity.) Substituting (2.27) into (2.24) we get

$$H(z) = \kappa_n \cdot \frac{b_n(z)g(z) + zf(z)\tilde{a}_n(z)}{a_n(z)g(z) + zf(z)\tilde{b}_n(z)} = \sum_{k=0}^{n} h_k z^k + O(z^{n+1}). \tag{2.28}$$

Since every rational system after repeated application of the Schur procedure has the above representation for any n, where $f(z)/g(z)$ is a unique rational bounded function as in (2.27), we can make use of the degree constraint of $H(z)$ in (2.28) to obtain this unknown bounded function. Towards this, notice that the formal degree of both the numerator and denominator of (2.28) is $n + p$, and to respect the ARMA(p, q) nature of $H(z)$, we first equate the denominator coefficients of z^{p+1}, z^{p+2}, $\cdots$, z^{p+n} to zero. However, as shown in [18], equating the coefficients of z^{p+1}, z^{p+2}, $\cdots$, z^{p+n} in the denominator to zero implies that the respective coefficients in the numerator are also zeros. As a result, we obtain n equations from the denominator coefficients of z^{p+1}, z^{p+2}, $\cdots$, z^{p+n}, and $p - q$ equations from the remaining numerator coefficients of z^{q+1}, $\cdots$, z^p. Thus we have $n + p - q$ equations and $2p$ unknowns g_k, $k = 1 \rightarrow p$ and f_k, $k = 0 \rightarrow p - 1$. Clearly the minimum value of n is given by $n = p + q$ and in that case the resulting $2p$ equations in $2p$ unknowns can be represented in matrix form as

$$\mathbf{A}\mathbf{x} = \mathbf{b} \tag{2.29}$$

where

$$\mathbf{A} \triangleq \left[\begin{array}{ccccc|ccccc} a_{p+q} & 0 & \cdots & 0 & 0 & b_0^* & 0 & \cdots & 0 & 0 \\ a_{p+q-1} & a_{p+q} & \cdots & 0 & 0 & b_1^* & b_0^* & \cdots & 0 & 0 \\ \vdots & \vdots & \vdots & \vdots & \vdots & \vdots & \vdots & \vdots & \vdots & \vdots \\ a_{q+2} & a_{q+3} & \cdots & a_{p+q} & 0 & b_{p-2}^* & b_{p-3}^* & \cdots & b_0^* & 0 \\ a_{q+1} & a_{q+2} & \cdots & a_{p+q-1} & a_{p+q} & b_{p-1}^* & b_{p-2}^* & \cdots & b_1^* & b_0^* \\ \vdots & \vdots & \vdots & \vdots & \vdots & \vdots & \vdots & \vdots & \vdots & \vdots \\ a_1 & a_2 & \cdots & a_{p-1} & a_p & b_{p+q-1}^* & b_{p+q-2}^* & \cdots & b_{q+1}^* & b_q^* \\ \hline b_0 & b_1 & \cdots & b_{p-2} & b_{p-1} & a_{p+q}^* & a_{p+q-1}^* & \cdots & a_{q+2}^* & a_{q+1}^* \\ 0 & b_0 & \cdots & b_{p-3} & b_{p-2} & 0 & a_{p+q}^* & \cdots & a_{q+3}^* & a_{q+2}^* \\ \vdots & \vdots & \vdots & \vdots & \vdots & \vdots & \vdots & \vdots & \vdots & \vdots \\ 0 & 0 & \cdots & b_q & b_{q+1} & 0 & 0 & \cdots & a_p^* & a_{p-1}^* \\ 0 & 0 & \cdots & b_{q-1} & b_q & 0 & 0 & \cdots & a_{p+1}^* & a_p^* \end{array}\right], \quad (2.30)$$

$$\mathbf{x} \triangleq \left[\begin{array}{ccccc|cccc} g_p & g_{p-1} & \cdots & g_2 & g_1 & f_{p-1} & f_{p-2} & \cdots & f_1 & f_0 \end{array}\right]^T \quad (2.31)$$

and

$$\mathbf{b} \triangleq \left[\begin{array}{cccccc|ccc} 0 & 0 & \cdots & 0 & a_{p+q} & \cdots & a_{p+1} & b_p & b_{p-1} \cdots & b_{q+1} \end{array}\right]^T . \quad (2.32)$$

Here a_k, b_k, $k = 0 \rightarrow p+q$ represent the coefficients of the $p+q$ degree Schur polynomials $a_{p+q}(z)$ and $b_{p+q}(z)$ respectively, i.e.,

$$a_{p+q}(z) = a_0 + a_1 z + a_2 z + \cdots + a_{p+q} z^{p+q} , \quad (2.33)$$

and

$$b_{p+q}(z) = b_0 + b_1 z + b_2 z + \cdots + b_{p+q} z^{p+q} . \quad (2.34)$$

Note that $p+q$ represents the minimum value for the available data points n, and if a larger number of such data is available, then these equations can be modified to accomodate that situation leading to an overdetermined system of equations in (2.29). At the correct stage, (2.29) is guaranteed to have a unique solution that results in a bounded function for $f(z)/g(z)$, and the unknown system parameters of $H(z)$ can be expressed in terms of the g_k's and f_k's so obtained. In fact, from (2.28), with

$$H(z) = \frac{Q(z)}{P(z)} = \frac{Q_0 + Q_1 z + \cdots + Q_q z^q}{P_0 + P_1 z + \cdots + P_p z^p} = \sum_{k=0}^{p+q} h_k z^k + O(z^{p+q+1}) \quad (2.35)$$

we get

$$P_k = \sum_{i=0}^{k} a_i g_{k-i} + \sum_{i=0}^{k-1} b^*_{n-i} f_{k-1-i}\,, \quad k = 0 \to p \tag{2.36}$$

and

$$Q_k = \kappa_{p+q} \left(\sum_{i=0}^{k} b_i g_{k-i} + \sum_{i=0}^{k-1} a^*_{n-i} f_{k-1-i} \right)\,, \quad k = 0 \to q\,. \tag{2.37}$$

Clearly, stability of $H(z)$ and the interpolation property follows from the bounded character of $d_{n+1}(z)$, and since $P(z)$ and $Q(z)$ are computed without involving any spectral factorization, the nonminimum phase characteristics of $H(z)$ if any is also preserved here.

Finally, to show the uniqueness of the ARMA(p,q) form in (2.35), the degree reduction possibility through common factor cancellation in its numerator and denominator must be ruled out. To see this, let $d_{n+1}(z) = f(z)/g(z)$ represent any rational bounded function in (2.28). Then from (2.19) and (2.28), since the denominator $P(z) = a_n(z) + z d_{n+1}(z)\tilde{b}_n(z)$ is strict Hurwitz, any such common zero between $P(z)$ and $Q(z) = b_n(z) + z d_{n+1}(z)\tilde{a}_n(z)$ must be outside the unit circle. Let z_0 represent such a common zero. Then $|z_0| > 1$, and from $P(z_0) = Q(z_0) = 0$, it is easy to show that

$$|d_{n+1}(z_0)| > 1\,. \tag{2.38}$$

On the other hand, referring back to $P(z_0) = 0$, we have

$$z_0 d_{n+1}(z_0) = -\frac{b_n(z_0)}{\tilde{a}_n(z_0)}\,, \tag{2.39}$$

and since $\tilde{a}_n(z)$ is free of zeros in $|z| \geq 1$, the function $b_n(z)/\tilde{a}_n(z)$ is analytic in $|z| \geq 1$ and it is bounded by unity on the unit circle. Thus by maximum modulus [15], $b_n(z)/\tilde{a}_n(z)$ is bounded by unity everywhere in $|z| \geq 1$, and in particular from (2.39), at $z = z_0$, we have

$$|z_0 d_{n+1}(z_0)| = \left| \frac{b_n(z_0)}{\tilde{a}_n(z_0)} \right| < 1\,,$$

or $|d_{n+1}(z_0)| < 1$, which contradicts (2.38), implying that the numerator and denominator factors in (2.35) are free of any such common factors outside the unit circle, and hence in the entire z-plane. This proves the uniqueness of the degree reduction condition through the procedure described in (2.29)–(2.32).

Equations (2.27)–(2.37) can be implemented provided p and q are known. Usually the model order (p,q) is unknown, and that will have to be evaluated from the given data. As we show below, the invariant characteristics of the rational bounded function $d_{n+1}(z)$ in (2.26), together with the Schur update rule in (2.12) can be used to determine the model order.

2.2.3 Model Order Selection

Having determined $d_{p+q+1}(z) = f(z)/g(z)$ as in (2.29)–(2.32), the bounded function $d_{p+q+2}(z)$ at the next stage ($n = p+q+1$) can be evaluated in a similar manner from the Schur polynomials $a_{p+q+1}(z)$ and $b_{p+q+1}(z)$. In fact, letting

$$d_{p+q+2}(z) \triangleq \frac{c(z)}{e(z)} = \left(\sum_{k=0}^{p-1} c_k z^k\right) \Big/ \left(\sum_{k=0}^{p} e_k z^k\right) \tag{2.40}$$

from (2.28), we also have

$$H(z) = \kappa_{p+q+1} \cdot \frac{b_{p+q+1}(z)e(z) + z\tilde{a}_{p+q+1}(z)c(z)}{a_{p+q+1}(z)e(z) + z\tilde{b}_{p+q+1}(z)c(z)} \tag{2.41}$$

and as before $e(z)$ and $c(z)$ can be evaluated by equating the coefficients of z^{p+1}, z^{p+2}, $\cdots$, z^{2p+q+1} in the denominator and z^{q+1}, z^{q+2}, $\cdots$, z^p in the numerator to zero[4]. Once again, these equations possess a unique solution at the correct stage for the unknowns e_k, $k = 1 \to p$, c_k, $k = 0 \to p-1$, (with $e_0 = 1$), and they result in a bounded function in (2.40). Notice that both these bounded functions $d_{p+q+1}(z)$ and $d_{p+q+2}(z)$ are of degree p, have the same form as in (2.27), and are related through the Schur rule as in (2.12). $d_{p+q+2}(z)$ makes use of additional information h_{p+q+1} about the system, through the new Schur polynomials. Substituting these two bounded functions into (2.12) and simplifying, we obtain

$$\frac{f(z)}{g(z)} = \frac{f_0 e(z) + zc(z)}{e(z) + z f_0^* c(z)}. \tag{2.42}$$

Equation (2.42) relates the coefficients of the bounded functions at two consecutive stages, and equating the ratios of like powers on both sides of (2.42) and rearranging, we obtain the conditions

$$\epsilon_k(p,q) = 0\,, \quad k = 0 \to p-1\,,$$

where

$$\epsilon_0(p,q) \triangleq f_0 e_p + c_{p-1} \tag{2.43}$$

and

$$\epsilon_k(p,q) \triangleq \frac{f_0 e_k + c_{k-1}}{e_k + f_0^* c_{k-1}} - \frac{f_k}{g_k}\,, \quad k = 1 \to p-1\,. \tag{2.44}$$

[4]Although this results in $(2p+1)$ equations in $2p$ unknowns, since the coefficient of z^{2p+q+1} is the same as (2.43), the remaining $2p$ equations are implemented in our computations.

These conditions are a direct consequence of (2.26), and reflect the ARMA(p,q) nature of the problem. Since the first stage where (2.43) and (2.44) are satisfied occurs at the correct stage, by updating p and q sequentially starting with $p \geq 1$ and $q \leq p$, the true model order can be found as the smallest integers p and q that satisfy

$$\epsilon_0(p,q) = 0\,,$$

or, more genreally

$$\epsilon(p,q) = \sqrt{\sum_{k=0}^{m} |\epsilon_k(p,q)|^2} = 0\,. \tag{2.45}$$

The key feature of a rational system – its degree – is exploited here in determining the true model order and system parameters.

The nonminimum phase stable rational transfer function examples in Figs. 1–2 highlight all important aspects of the algorithm described in this report. The unknown system is assumed to be ARMA(n,m) with $n \geq m$, and initialization begins with $n = 1$, $m = 0$. Preparation of the given impulse response sequence h_k, $k = 0 \rightarrow n+m+1$, is first carried out to generate $d_k = h_k/\kappa_{n+m+1}$, $k = 0 \rightarrow n+m+1$ as in (2.22)–(2.23). Computation of the Schur polynomials $a_{n+m+1}(z)$, $b_{n+m+1}(z)$ using (2.16)–(2.17) and (2.20)–(2.21), followed by those of the bounded functions $d_{n+m+1}(z) = f(z)/g(z)$ and $d_{n+m+2}(z) = c(z)/e(z)$ then allow $\epsilon_0(n,m)$ and $\epsilon(n,m)$ to be evaluated using (2.43), (2.45), *provided both* $d_{n+m+1}(z)$ and $d_{n+m+2}(z)$ exist as bounded functions. The heavy dots on all curves in Figs. 1(c)–2(c) indicate the presence of such a stage (n,m), and if such is not the case that particular stage is skipped and the indices n and m are updated. Notice that $\epsilon_0(n,m)$ and $\epsilon(n,m)$ are guaranteed to exist at the correct stage $n = p$ and $m = q$, and since the first place where $\epsilon_0(n,m)$ and $\epsilon(n,m)$ equal zero also occurs at the correct stage, sequential updating of n and m continues until substantial relative minima in the values of $\epsilon_0(n,m)$ and $\epsilon(n,m)$ are observed to occur for the first time. The corresponding pair (n,m) is then identified as the model order (p,q) and the system parameters are computed from (2.35)–(2.37). Finally, to facilitate comparison, the exact magnitude $|H(e^{j\theta})|$ and its reconstructed counterpart (dotted) are plotted in Figs. 1(a)–2(a). Similarly, the exact phase $\phi(\theta)$ and the reconstructed phase (dotted) are plotted in Figs. 1(b)–2(b).

Although the theoretical development in section III assumes $p \geq q$, as the MA(5) example in Fig. 2 shows, every case where $q > p$ can be detected as an ARMA(q,q) system. This means of course that some of the reconstructed coefficients in the denominator are filled in automatically as zeros, to raise the denominator degree to q.

2.3 Stable Rational Approximation of Nonrational Systems

A nonrational system has a transfer function that, unlike the rational systems, cannot be expressed as the ratio of two polynomials of finite degree. If such a system is stable, then it admits a power series expansion in $|z| < 1$, and the problem is to represent this by a rational system in some optimal manner. As remarked in the introduction, although Padé approximations can achieve this goal, such approximations need not guarantee stability. Moverover, the Hankel matrices generated from the impulse response data has no particular rank invariant structure in this case. In this context, once again we can make use of (2.24) to obtain all stable rational solutions to this problem.

To start with notice that the Schur extraction principle in (2.12)–(2.13) is perfectly general and hence if $H(z)$ is nonrational, then the representation in (2.24) is still valid, where $d_{n+1}(z)$ in that case represents a nonrational bounded function. Interestingly, as remarked there, if $d_{n+1}(z)$ is replaced by any rational bounded function, we obtain a stable rational transfer function $H_r(z)$ that interpolates the given impulse response sequence $\{h_k\}_{k=0}^{n}$. This key observation can be used to determine interpolating rational systems with minimum degree.

Since Padé approximations preserve the optimal degree character, if such approximations are also stable, then they must follow from (2.24) for a specific rational bounded function $d_{n+1}(z)$. To determine such bounded functions, let $d_{n+1}(z) = f(z)/g(z)$ represent a degree m bounded function that when substituted into (2.24) generates an ARMA(p,q) Padé-approximation $H_r(z)$. Thus

$$H_r(z) = \frac{Q(z)}{P(z)} = \kappa_n \cdot \frac{b_n(z)g(z) + z\tilde{a}_n(z)f(z)}{a_n(z)g(z) + z\tilde{b}_n(z)f(z)} = \sum_{k=0}^{n} h_k z^k + O(z^{n+1}). \tag{2.46}$$

For (2.46) to represent the Padé approximation, we must have $p + q \leq n$, and once again to respect the ARMA(p,q) nature of $H_r(z)$, the polynomial $f(z)$ must be of degree $m-1$ and hence $g(z)$ must be of degree m. Thus the formal degrees of $P(z)$ and $Q(z)$ in (2.46) are $n+m$, provided $\delta(a_n(z)) = n$, and hence the coefficients of $z^{p+1}, \cdots, z^{n+m}$ in the denominator, and the coefficients of $z^{q+1}, \cdots, z^{n+m}$ in the numerator must be zeros. It can be shown that the coefficients of $z^{m+1}, \cdots, z^{n+m}$ in the numerator and denominator generate the same equations and hence this gives $n+(m-p)+(m-q) = n+2m-(p+q)$ equations in $2m$ unknowns. Since $n \geq p+q$, there are at least $2m$ equations and they can be used to solve for the unknowns. ¿From the above degree argument $m-p \geq 0$ and $m-q \geq 0$, or $m \geq max(p,q)$, and hence for a given p, q (with $p \geq q$), the least complex bounded function $d_{n+1}(z)$ is also of degree p. In that case, the desired bounded function $d_{n+1}(z)$ has exactly the same form as in (2.27), and the system of equations so obtained has the functional representation in (2.29)–(2.32). However, unlike the rational case, the system of equations so obtained need not yield a solution for $g(z)$ and $f(z)$, and even if a solution exists there, $g(z)$ so

obtained need not be strict Hurwitz, and further $f(z)/g(z)$ need not turn out to be a bounded function. However, for some p, q, if $f(z)/g(z)$ turns out to be a bounded function, then $H_r(z)$ in (2.46) represents a stable ARMA(p,q) Padé approximation to the given nonrational function. Thus every stable Padé approximation to the given data has the representation

$$H_r(z) = \frac{Q(z)}{P(z)} = \kappa_{p+q} \frac{b_{p+q}(z)g(z) + z\tilde{a}_{p+q}(z)f(z)}{a_{p+q}(z)g(z) + z\tilde{b}_{p+q}(z)f(z)} = \sum_{k=0}^{n} h_k z^k + O(z^{n+1}), \qquad (2.47)$$

where $n \geq p+q$, and $f(z)/g(z)$ represents a bounded function given by (2.29)–(2.32). We summarize the above observations as follows:

The necessary and sufficient condition for the existence of a stable ARMA(p,q) Padé approximation to the impulse response sequence $\{h_k\}_{k=0}^{p+q}$ is that the system of linear equations in (2.29)–(2.32) generated from the associated Schur polynomial coefficients yield a bounded solution of degree q for $f(z)/g(z)$ in (2.27). In that case, (2.35)–(2.37) and (2.47) represent the desired stable transfer function.

Interestingly, the above remarks raise the following question: Given an $H(z)$ that represents a stable (nonrational) system transfer function, does there always exist a stable ARMA(p,q) Padé approximation for some p and q? Clearly, if such a solution exists, then that must follow from (2.47) with $n \geq p+q$ for a rational bounded function $f(z)/g(z)$ of degree p, that is obtained by solving the system of equations in (2.29)–(2.32).

Although it is easy to show that the strict Hurwitz character of $g(z)$ must occur infinitely often, indicating the possibility of the desired bounded function in (2.46)–(2.47), unfortunately, nothing more specific can be said about the bounded character of $d_{n+1}(z) = f(z)/g(z)$. In fact, given h_k, $k = 0 \rightarrow n$, there might exist no stable Padé approximation, and, moreover, the lowest nontrivial stable rational approximation that matches the given data might be of ARMA(n,n) form which corresponds to $d_{n+1} \equiv 0$ in (2.24). However, so long as $f(z)/g(z)$ is chosen to be a rational bounded function in (2.46), it represents the class of all stable rational transfer functions that interpolate h_0, h_1, $\cdots h_n$. Thus even if stable Padé approximations and absent in a particular situation, by relaxing the Padé constraint, other stable rational approximations can be obtained.

Figs. 3–4 as well as our extensive computations involving nonrational systems containing logarithmic and essential singularities seem to indicate that stable Padé approximations always exist. In the simulations presented here, the original nonrational function $H(z)$ is used to compute h_k, $k = 0 \rightarrow p+q$, and it is first 'prepared' to generate d_k, $k = 0 \rightarrow p+q$, as in (2.22)–(2.23) and thereby the Schur polynomials $a_{p+q}(z)$ and $b_{p+q}(z)$. From the above theorem, since a stable ARMA(p,q) Padé approximation to this data must follow from (2.47) for a bounded solution of

$f(z)/g(z)$ given by (2.29)–(2.32), those equations are verified for such a solution, and the indices are updated in a sequential manner. The heavy dots in Figs 3(c)–4(c) indicate the presence of such a stage, where (2.29)–(2.32) yield a bounded solution for $d_{p+q+1}(z) = f(z)/g(z)$ that results in a stable Padé approximation. Further, if the two consecutive rational functions $d_{p+q+1}(z)$ and $d_{p+q+2}(z)$ turn out to be bounded and are related as in the Schur algorithm, then $\epsilon_0(p,q)$, $\epsilon_k(p,q)$ will be zero. When $H(z)$ is known in advance, the percent spectral error

$$\eta(p,q) = \sup_{\theta} \frac{\left||H(e^{j\theta})|^2 - |H_r(e^{j\theta})|^2\right|}{|H(e^{j\theta})|^2} \tag{2.48}$$

also may be used for model order selection. Notice that Fig. 4 represents a transcendental nonminimum phase system (zero at the origin) with a logarithmic singularity at $z = 1$. Nevertheless, as seen from Figs. 4(a)–(c), the ARMA(14,4) Padé approximation is stable and preserves the nonminimum phase character of the original system. The abundance of stable Padé approximations are evident in Figs 4(c)–5(c). Nevertheless a rigorous proof is still lacking in the general case regarding the bounded character of $f(z)/g(z)$ for some p, q, and the issue remains unresolved.

2.4 Conclusions

This report investigates the problem of obtaining all stable rational solutions that interpolate the given partial impulse response sequence by making use of the well known theory of bounded (Schur) functions. In this context, a new test criterion is developed to determine the model order of rational systems, and thereby determine their system parameters from the given impulse response sequence. The theory developed is further utilized to obtain the necessary and sufficient conditions for stable Padé approximations of nonrational systems. A practical algorithm is developed that translates the stability condition into the bounded character of a rational function generated from a set of linear equations obtained from the Schur polynomial coefficients associated with the given impulse response sequence. Interestingly, since the present technique does not make use of any factorization procedure, the nonminimum phase characteristics of the original system are preserved here.

2.5 References

[1] G. A. Baker, Jr., *Essentials of Padé Approximants*, New York: Academic Press, 1975.

[2] W. B. Jones and W. J. Thron, *Continued Fractions: Analytic Theory and Applications*, Cambridge University Press, 1984.

[3] Y. T. Chan and J. C. Wood, "A new order determination technique for ARMA processes," *IEEE Trans. Acoust., Speech, Signal Processing*, vol. ASSP-32, no. 3, pp. 517–521, June 1984.

[4] J. J. Fuchs, "ARMA order estimation via matrix perturbation theory," *IEEE Trans. Autom. Control*, vol. AC-32, no. 4, pp. 358–361, April 1987.

[5] I. Schur, "On power series which are bounded in the interior of the unit circle," Parts I and II, in *I. Schur Methods in operator theory and signal processing* ed. by I Gohberg, pp.31-88, Birkhauser, Boston, 1986.

[6] H. Dym, "*J-Contractive Matrix Functions, Reproducing Kernel Hilbert Spaces and Interpolation*, No.71 in CBMS regional conference series, Providence: American Math. Soc., 1989.

[7] P. Dewilde and H. Dym, "Schur Recursions, Error Formulars, and Convergence of Rational Estimators for Stationary Stochastic Sequences," *IEEE Trans. Informat. Th.*, vol.27, pp446-461, July 1981.

[8] Ph. Delsarte, Y. Genin, and Y. Kamp, "On the role of the Nevanlinna-Pick Problem in Circuit Theory and Design," *Circuit Th. Appl.*, vol.9, pp177-187, 1981.

[9] D. Alpay, P. Dewilde, and H. Dym, "On the Existance and Construction of Solutions to the Partial Lossless Inverse Scattering Problem with Applications to Estimation Theory," *IEEE Trans. informat. Th.*, vol.35, pp.1184-1205, Nov. 1989.

[10] S. Y. Kung and D. W. Lin, "Optimal Hankel Norm Model Reductions: Multivariable Systems," *Int. J. Control*, vol.39, no.6, pp.1115-1193, 1984.

[11] V. M. Adamjan, D. Z. Arov, and M. G. Krein, "Analysis Properties of Schmidt Pairs for a Hankel Operator and the Generalized Schur-Takagi Problem," *Math. USSR. Sbornik*, vol.15, no.1, pp31-73, 1971.

[12] T. Zhou and H. Kimura, "Time domain identification for robust control," *System & Control Letters*, vol.20, pp167-178, 1993.

[13] A. M. King, U. B. Desai and R. E. Skelton, "A Generalized Approach to q-Markov Covariance Equivalent Realizations for Discrete Systems," *Automatica*, vol.24, No.4, pp.507-515, 1988.

[14] H. Kimura, "Positive partial realization of covariance sequences," *Modeling, Identification and Robust Control*, C. I. Byrnes and A. Lindquist. Eds. Amsterdam: North-Holland, 1987, pp. 499-513.

[15] P. Dienes, *The Taylor Series*, New York: Dover Publications, 1957.

[16] M. Marden, *The Geometry of the Zeros of a Polynomial in a Complex Variable*, Amer. Math. Soc., Math. Survey, no. 3, 1949.

[17] S. U. Pillai, T. I. Shim, and D. C. Youla, "A new technique for ARMA-system identification and rational approximation," *IEEE Trans. Signal Processing*, vol. SP-41, no. 3, pp. 1281–1304, March 1993.

[18] W. C. Lee, "Identification of Nonminimum Phase Stable Systems," Ph.D Dissertation, Department of Electrical Engineering, Polytechnic University, Brooklyn, New York, Jan 1995.

[19] D. C. Youla, "The FEE: A new tunable high-resolution spectral estimator," Part I, Technical note, no. 3, Department of Electrical Engineering, Polytechnic Institute of New York, Brooklyn, New York, 1980: also RADC Rep. RADC-TR-81-397, AD A114996, February 1982.

[20] D. C. Youla, "Two observations regarding First-quadrant Causal BIBO stable Digital Filters," *Proc. IEEE*, vol. 78, no. 4, pp. 598–603, April 1990.

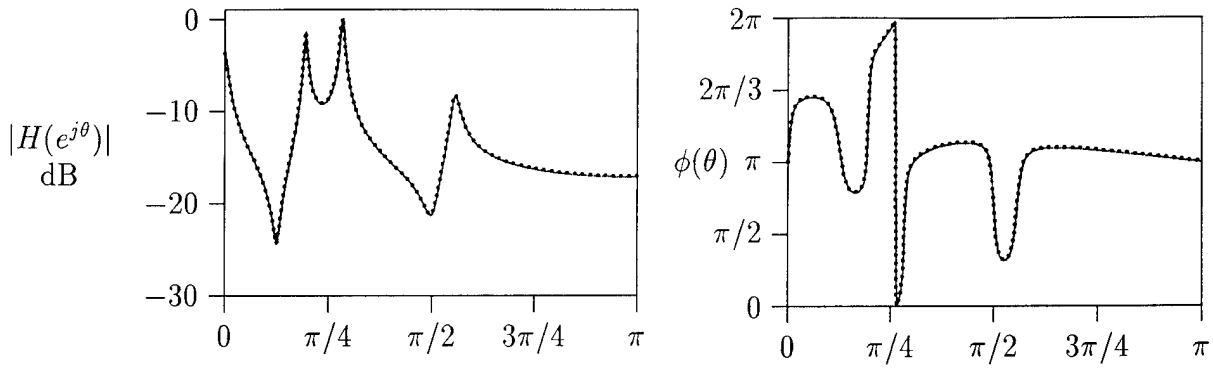

(a) Original/reconst. magnitude.

(b) Original/reconst. phase.

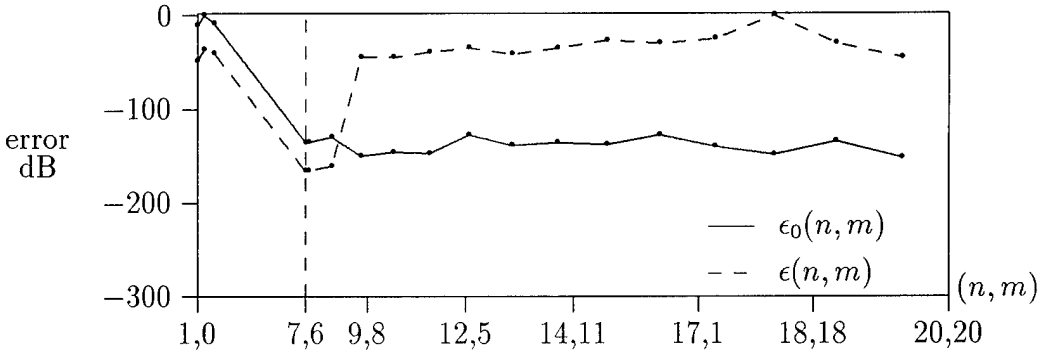

(c) Test criteria for model order selection

Figure 1: Reconstruction of a nonminimum phase ARMA(7,6) model from its partial impulse response sequence. The original model corresponds to

$$H(z) = \frac{0.602 - 2.206z + 4.160z^2 - 4.952z^3 + 4.366z^4 - 2.721z^5 + 0.888z^6}{1.0 - 3.511z + 6.438z^2 - 8.052z^3 + 7.875z^4 - 6.018z^5 + 3.186z^6 - 0.888z^7}.$$

Poles of $H(z)$ are at $1.02\angle 0°$, $1.01\angle \pm 35°$, $1.01\angle \pm 51°$ and $1.03\angle 100°$.
Zeros of $H(z)$ are at $1.02\angle \pm 22°$, $0.769\angle \pm 43°$ and $1.05\angle \pm 90°$.
The reconstructed model is given by

$$H_r(z) = \frac{0.602 - 2.206z + 4.160z^2 - 4.952z^3 + 4.366z^4 - 2.721z^5 + 0.888z^6}{1.0 - 3.511z + 6.438z^2 - 8.052z^3 + 7.875z^4 - 6.018z^5 + 3.186z^6 - 0.888z^7}.$$

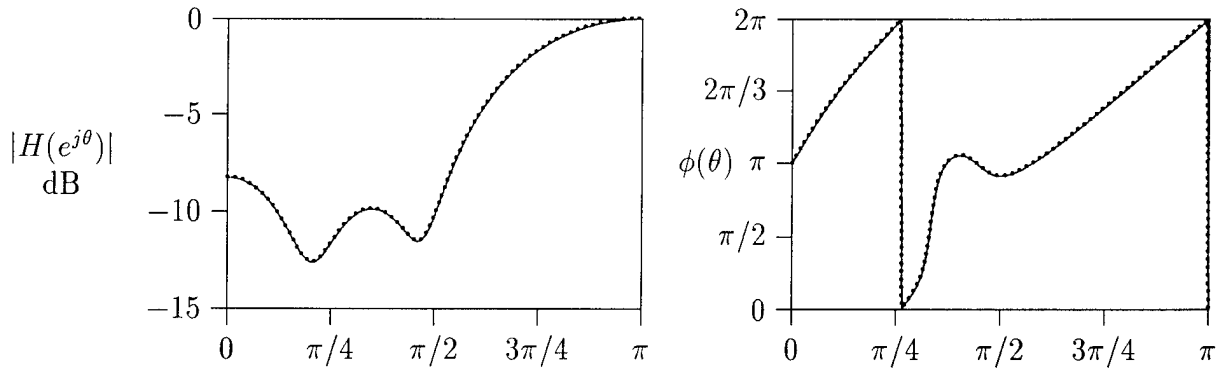

(a) Original/reconst. magnitude. (b) Original/reconst. phase.

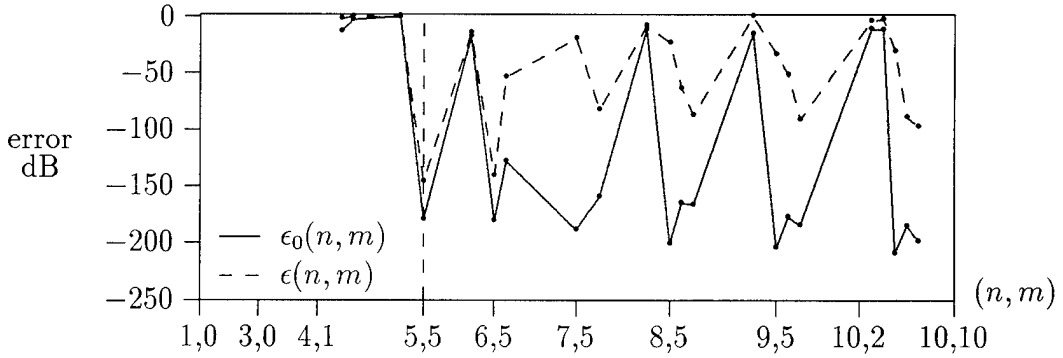

(c) Test criteria for model order selection

Figure 2: Reconstruction of an MA(5) model from its partial impulse response sequence. The original model corresponds to

$$H(z) = 0.8704 - 2.4714z + 3.5782z^2 - 3.6560z^3 + 2.0357z^4 - 1.0z^5 .$$

Zeros of $H(z)$ are at $0.667\angle 0°$, $0.952\angle \pm 60°$ and $1.2\angle \pm 80°$.
The reconstructed model is given by

$$H_r(z) = \frac{0.8704 - 2.4714z + 3.5782z^2 - 3.6560z^3 + 2.0357z^4 - 1.0z^5}{1 + 2.1 \times 10^{-17}z - 1.5 \times 10^{-16}z^2 + 4.1 \times 10^{-15}z^3 + 2.6 \times 10^{-14}z^4 + 7.2 \times 10^{-14}z^5} .$$

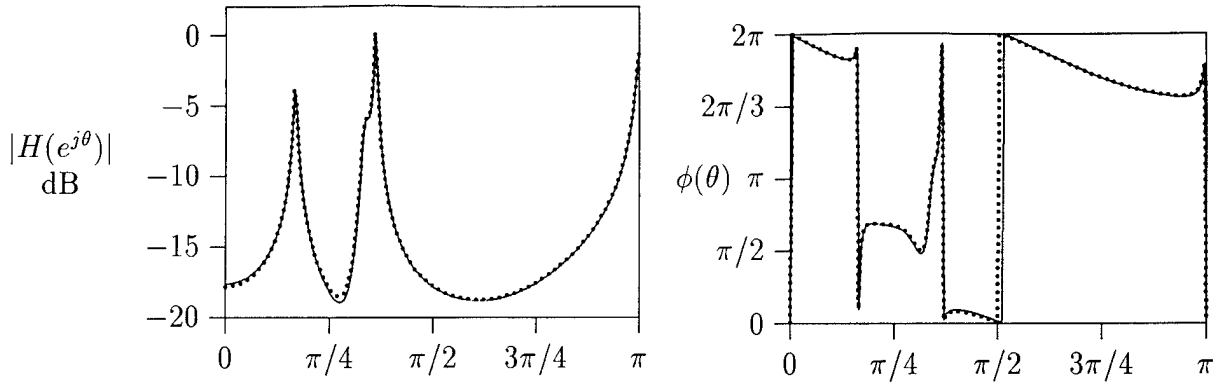

(a) Original/approx. magnitude.

(b) Original/approx. phase.

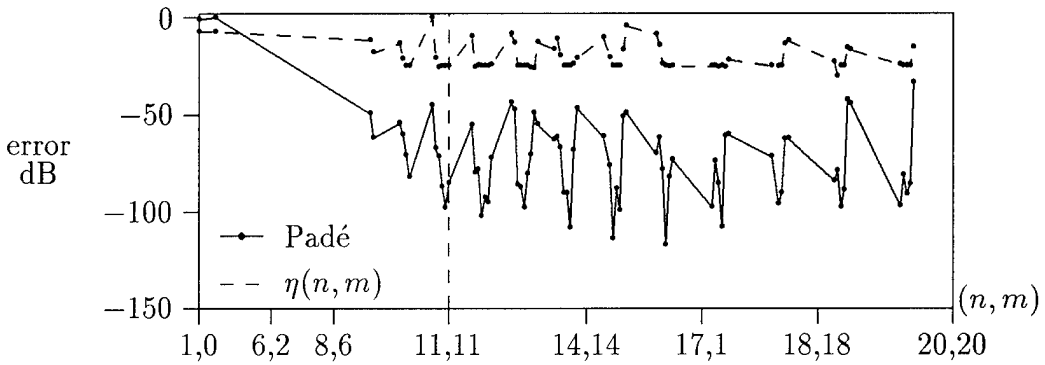

(c) Test criteria for model order selection

Figure 3: Rational approximation of a nonrational system. The original nonrational transfer function is given by

$$H(z) = H_1(z)e^{-z} + H_2(z)e^{-(z-1)}$$

where

$$H_1(z) = \frac{1.1 + z}{1.02 - 1.75z + z^2}\,,\quad H_2(z) = \frac{1.04 - 1.31z + z^2}{1.09 - 0.91z + 1.06z^2 + 1.03z^3 - 0.86z^4 + z^5}\,.$$

The stable Padé approximation ARMA(11,11) model is given by $H_r(z) = B_m(z)/A_n(z)$, where

$$\begin{aligned} A_n(z) &= 1 - 2.111z + 2.351z^2 - 0.265z^3 - 1.869z^4 + 2.459z^5 - 1.078z^6 \\ &\quad +0.119z^7 + 0.228z^8 + 0.0557z^9 + 0.0059z^{10} + 0.00026z^{11}\,, \\ B_m(z) &= 3.571 - 9.609z + 15.720z^2 - 12.974z^3 + 7.440z^4 - 2.243z^5 + 1.227z^6 \\ &\quad -0.555z^7 + 0.126z^8 - 0.0188z^9 + 0.0016z^{10} - 0.00006z^{11}\,. \end{aligned}$$

Zeros of $A_n(z)$ are at $1.01\angle\pm30°$, $1.007\angle\pm78.9°$, $1.0256\angle\pm60°$, $7.29\angle\pm162°$, $8.066\angle\pm 45°$ and $1.019\angle180°$. Zeros of $B_m(z)$ are $0.782\angle \pm 53.2°$, $1.107\angle \pm 55°$, $2.309\angle \pm 123°$, $6.512\angle \pm 67.5°$, $10.17\angle \pm 24°$ and $3.37\angle0.0°$.

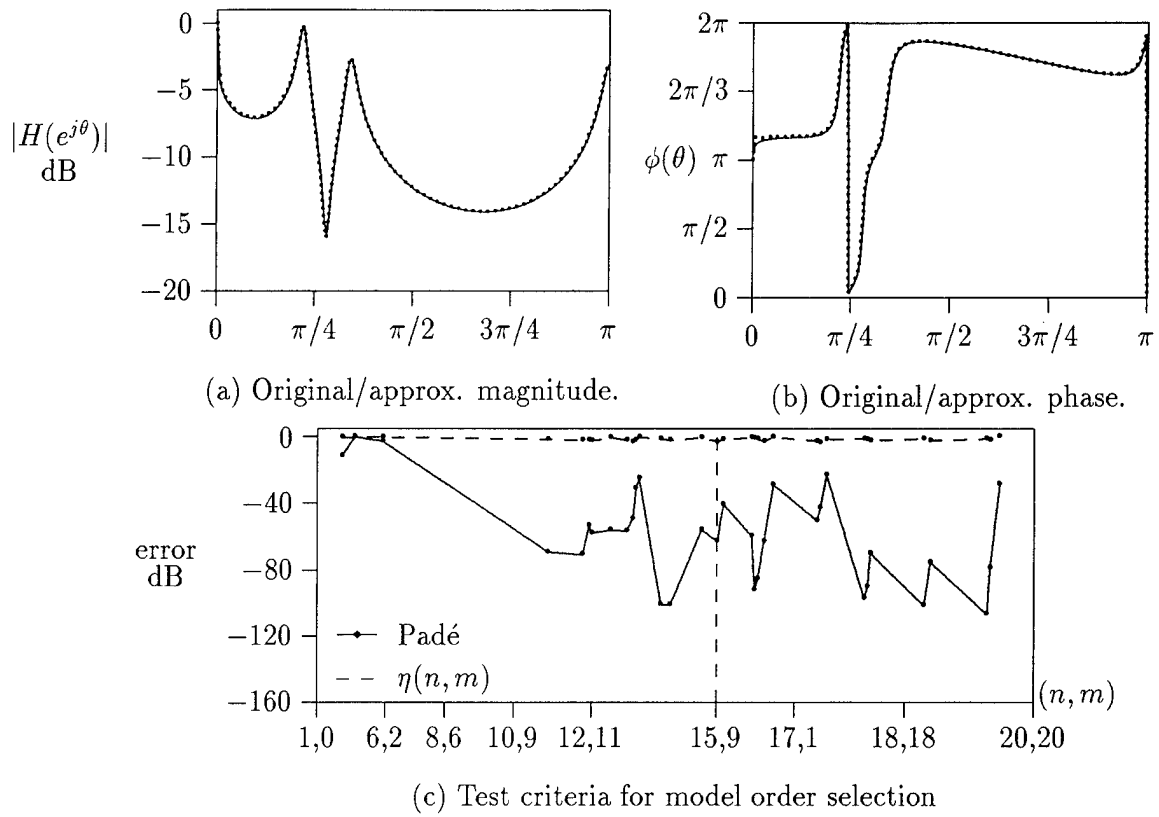

(a) Original/approx. magnitude.

(b) Original/approx. phase.

(c) Test criteria for model order selection

Figure 4: Rational approximation of a nonrational system with a logarithmic singularity at $z = 1$. The original nonrational transfer function is given by

$$H(z) = \frac{0.797 - 1.036z + 0.829z^2}{1 - 1.470z + 0.946z^2 + 0.841z^3 - 1.277z^4 + 0.829z^5} ln(1 - z)$$

Poles of $H(z)$ are at $1.03\angle \pm 39.6°$, $1.04\angle \pm 61.2°$ and $1.05\angle 180°$. Zeros of $H(s)$ are at $0.98\angle \pm 50.4°$.

The stable Padé ARMA(14,4) model is given by $H_r(z) = B_m(z)/A_n(z)$, where

$$\begin{aligned} A_n(z) &= 1 - -2.8536z + 3.3370z^2 - 0.9590z^3 - 2.1421z^4 + 2.9183z^5 - 1.5714z^6 \\ &\quad +0.2655z^7 0.0188z^8 + 0.0053z^9 0.0022z^{10} 0.0011z^{11} + 5.21 \times 10^{-4} z^{12} \\ &\quad +2.11 \times 10^{-4} z^{13} + 5.35 \times 10^{-5} z^{14}, \\ B_m(z) &= -0.0009 - 0.7955z + 1.7398z^2 - 1.7455z^3 + 0.73305z^4 . \end{aligned}$$

Zeros of $B_m(z)$ are at $0.98\angle \pm 50.4°$, $1.1323\angle 0.0°$ and $0.0011\angle 180.0°$.

3. Stacked Piezoceramic Actuators for Active Damping

3.1 Introduction

Utilization of active materials for vibration damping is recently receiving increased attention [1–6,25]. Research and development of completely integrated structures with embedded actuators, sensors, signal processing, and control systems are of prime interest. Different electroactive materials such as piezoceramics, shape memory alloys, electrorheological fluids, polymer biomaterials, and magnetorestrictive materials are being considered for such purposes. Piezoelectric ceramics are effective distributed strain actuators as well as sensors due to their high stiffness, good linearity, ease of integration, low temperature sensitivity, and relatively low noise. In this report, stacked piezoceramics are mainly considered for actuation purposes. Also, piezoceramics with interdigitated electrodes are considered [8,9]. Dynamical models of stacked piezoceramics are reported. Several experimental setups (ranging from beams and plates to multi-link flexible manipulators) have been developed to study modeling and control of smart structures at the CRRL.

One of the main issues in smart structures is the control system. Foremost in the design of advanced control systems is the need to satisfy performance specifications. In fact, one often sacrifices stability margin or accepts conditionally stable systems in order to realize superior performance. So one should begin with an optimal solution according to some measure. In the present work, an H_2 measure is considered. When the optimal solution exceeds specifications, the cost functional can be increased and the increment traded for an improvement in stability margin. That is, one should maximize stability margin subject to a constraint on the H_2-norm cost increment. When the stability margin obtained in this way is not adequate, then one must use a different controller for different operating profiles of the plant: typically, one should not give up performance just for the sake of operating with a single fixed controller when high performance is required. In order to attain an analytical solution to this fundamental tradeoff problem, the approximate measure of stability margin chosen is also a quadratic cost function. A complete derivation of the results for the advocated control system is given in [20].

This new control design methodology for tradeoffs between stability margin and performance is applied to vibration damping and pointing of smart structures. These systems do provide nice benchmark problems in control system design. The aforementioned control design methodology is applied to a flexible pointing system with embedded active materials and experimental results are presented to show the efficacy of the control design methodology and the added advantage of utilization of active materials.

3.2 Stacked Piezoceramic Elements

In this section, the dynamical model of stacked piezoceramic elements (e.g., plates, discs, etc.) attached electrically in parallel is developed. A typical stack of discs is

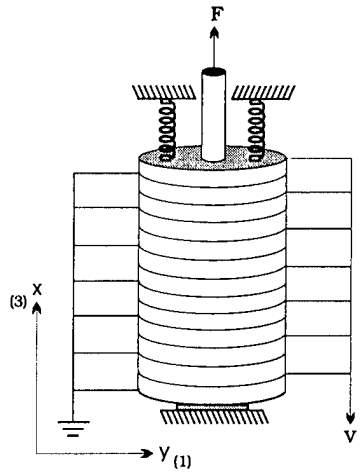

Figure 3.1: A stack of N-piezoceramic discs.

shown in Figure 3.1 where the piezoceramic elements are assumed to be polarized through their thickness. The electric work done by each element of the stack is derived to generate the dynamical model and to calculate the force generated by the stack.

The strain through the piezoelectric ceramic is expressed as

$$S = \begin{bmatrix} S_1 & S_2 & S_3 & S_4 & S_5 & S_6 \end{bmatrix}' = L_u u \tag{3.1}$$

where $(\cdot)'$ denotes the transpose, L_u is a 6×3 differential operator, and $u = [u_x \;\; u_y \;\; u_z]'$ is a 3×1 displacement vector.

The constitutive relation between the stress (T), strain (S), electric field (E), and electric charge distribution (D) in each of the piezoceramic elements is given by

$$\begin{bmatrix} T \\ D \end{bmatrix} = \left[\begin{array}{c|c} c^E & -e' \\ \hline e & \epsilon^s \end{array}\right] \begin{bmatrix} S \\ E \end{bmatrix} \tag{3.2}$$

where c^E is the stiffness matrix of the piezoceramic taken at constant electric field, ϵ^s is the matrix of dielectric constants taken at constant strain, and e is the matrix of material constants of the piezoceramic. All quantities are taken with respect to a local coordinate system pertaining to the direction of polarization.

The kinetic and potential energies of an element in the piezoceramic stack are given respectively as

$$T = \frac{1}{2}\rho_s \int_{\Omega_s} \dot{u}'\dot{u} \; d\Omega, \quad \text{and} \quad U = \frac{1}{2}\int_{\Omega_s} S'T \; d\Omega \tag{3.3}$$

where ρ_s is the mass volume density of the piezoceramic element and Ω_s denotes the spatial boundary of the section of the piezoceramic.

Replacing T by its equivalent from Eq.(3.2) simplifies the expression for the potential energy into

$$U = \frac{1}{2}\int_{\Omega_s}(S'c^E S - S'e'E)d\Omega. \tag{3.4}$$

The electric work done by the charge in each element of the stack is expressed as

$$W_e = \frac{1}{2}\int_{\Omega_s} E'D \ d\Omega. \tag{3.5}$$

Replacing D in the above equation by its value in Eq. (3.2) yields

$$W_e = \frac{1}{2}\int_{\Omega_s} E'eS \ d\Omega + \frac{1}{2}\int_{\Omega_s} E'\epsilon^s E \ d\Omega \tag{3.6}$$

where the first term signifies the actuation capability and can be expanded as

$$W_{act} = \frac{V}{2t_p}\int_{\Omega_s}(e_{31}S_1 + e_{32}S_2 + e_{33}S_3)\, d\Omega. \tag{3.7}$$

where the first subscript refers to the direction of the electric field and the second refers to the direction of the strain. The 3-direction is the direction of polarization (here corresponding to the x-direction), the 2-direction corresponds to z and the 1-direction corresponds to y. Note that $S_4 = S_5 = S_6 = 0$ signifying the absence of shear stresses.

For brevity, the piezoceramic elements are assumed to be identical and of a simple geometry (e.g., discs or plates) in the following analysis. Furthermore, the average electric field through each of the elements can be expressed as[1]

$$E = \begin{bmatrix} 0 & 0 & \frac{V}{t_p} \end{bmatrix}' \tag{3.8}$$

where V is the applied voltage and t_p is the thickness of the piezoceramic element.

The dominant strain is in the direction of polarization (i.e., the 3- direction). Hence, one can assume that only S_3 is non-zero. It then follows from Eqs. (3.4) and (3.8) that

$$\begin{aligned} U &= \frac{1}{2}A_p c_{33}^E \int_a^{a+t_p} S_3^2 \ dx - \frac{VA_p e_{31}}{2t_p}\int_a^{a+t_p} S_3 \ dx \\ &= \frac{1}{2}A_p c_{33}^E \int_a^{a+t_p}\left(\frac{\partial}{\partial x}\, u_x(x,t)\right)^2 \ dx \\ &\quad -\frac{VA_p e_{31}}{2t_p}\int_a^{a+t_p}\left(\frac{\partial}{\partial x}u_x(x,t)\right) \ dx \end{aligned} \tag{3.9}$$

[1]We consider uniform field through the piezoceramic since thin elements are normally utilized. However, the non-uniform field may similarly be handled.

where a and $a + t_p$ are the spatial limits of the piezoceramic element along the x-axis and A_p is the area of the faces of each of the piezoceramic elements constituting the stack.

Similarly, the component of displacement of largest significance is u_3 (x-direction); therefore, by neglecting the displacements in other directions, the kinetic energy simplifies into

$$T = \frac{1}{2}\rho_s A_p \int_a^{a+t_p} \dot{u}_x^2(x,t)\ dx \tag{3.10}$$

Finally, the total kinetic and potential energies of the stack are obtained by summing up those of the individual piezoceramic elements given in Eqs. (3.9) and (3.10). Thereafter, Hamilton's principle may be invoked to derive the dynamics of the piezoceramic stacks[2]. Furthermore, a discretization of the distributed parameter model may be performed to obtain a lumped parameter description of the piezoceramic stacks. This may be achieved through an assumed mode approach on the displacement, i.e.,

$$u_x(x,t) = \sum_{i=1}^{m} \phi_i(x)\eta_i(t) \tag{3.11}$$

where m is the number of retained modes, the $\phi_i(x)$ are the mode shape functions and the $\eta_i(t)$ are the amplitude functions.

The following analysis establishes the level of force such piezoceramic stacks may generate. Neglecting all strains in other directions than the polarization direction, the work done by the actuator given in (3.7) can be simplified to

$$W_{act} = \frac{V A_p e_{33}}{2t_p} \int_a^{a+t_p} S_3 dx. \tag{3.12}$$

Approximating the strain through the length as a constant, it can be expressed as

$$S_3 = \frac{\Delta L}{L} \tag{3.13}$$

where L is the total length of the stack and ΔL is the change in length of the stack due to an applied electric field. Then the expression for the actuation capability of each element becomes

$$W_{act} = \frac{V A_p e_{33} \Delta L}{2L}. \tag{3.14}$$

Remark: the total actuation of the stack is $N \times W_{act}$.

[2]Tip mass energy and spring energy due to preload may also be added.

To compute the force generated by one element of the stack, consider the mechanical work done:

$$W = \int_{\Omega_s} F \cdot du \tag{3.15}$$

where $F = [F_x \; F_y \; F_z]$ is a three dimensional vector with

$$F_x = \int_{\Omega_z} \int_{\Omega_y} T_3 dy dz, \tag{3.16}$$

$$F_y = \int_{\Omega_z} \int_{\Omega_x} T_1 dx dz, \tag{3.17}$$

$$F_z = \int_{\Omega_y} \int_{\Omega_x} T_2 dx dy, \tag{3.18}$$

and Ω_x,Ω_y and Ω_z are the spatial domains of the piezoceramic element along the x, y and z axes respectively. In Eq. (3.15), u is the displacement vector which can be expressed in terms of the normal strains (in its local coordinates)

$$u = \left[\begin{array}{ccc} u_x & u_y & u_z \end{array} \right]' = \left[\begin{array}{ccc} S_3 x & S_1 y & S_2 z \end{array} \right]' \cdot \tag{3.19}$$

When the strain components are constant along their respective directions throughout the piezoceramic stack, du can be expressed as

$$du = \left[\begin{array}{ccc} S_3 dx & S_1 dy & S_2 dz \end{array} \right]' \cdot \tag{3.20}$$

Thus, the mechanical work becomes

$$W = \int_a^{a+t_p} F_x S_3 dx + \int_{\Omega_y} F_y S_1 dy + \int_{\Omega_z} F_z S_2 dz \cdot \tag{3.21}$$

Since the component of the force being considered (x-component) is much larger than the other two force components, Eq. (3.21) may be approximated by

$$W = \int_a^{a+t_p} F_x S_3 dx \cdot \tag{3.22}$$

Having a constant force F_x along the x-direction, it may be computed by equating the actuation energy to the mechanical energy to obtain

$$F_x = \frac{1}{2} A_p E e_{33} = \frac{V A_p e_{33}}{2t_p}. \tag{3.23}$$

This is the force due to each of the elements in the stack; therefore, the total force exerted by the stack is

$$F_x = \frac{NV A_p e_{33}}{2tp} \cdot \tag{3.24}$$

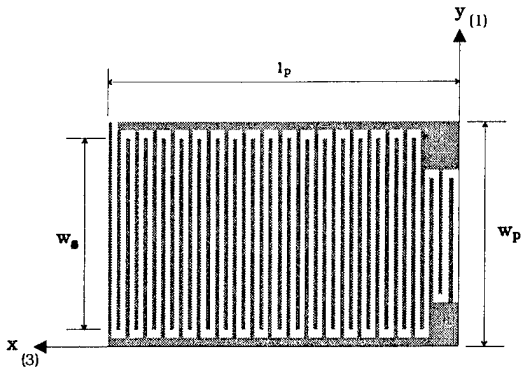

Figure 3.2: A piezoceramic plate with interdigitated electrodes.

If the stack is preloaded with a spring of stiffness c_s, e_{33} in Eq. (3.24) changes to $\hat{e_{33}}$ where

$$\hat{e_{33}} = \frac{c_T}{c_T + c_s} e_{33} \tag{3.25}$$

and

$$c_T = c_{33} \frac{N A_p}{L}. \tag{3.26}$$

3.3 Piezoceramic Plates With Interdigitated Electrodes

In this section, a model of a piezoceramic plate with interdigitated electrodes is presented. Fig. 3.2 gives the top-view of a piezoceramic plate with interdigitated electrodes. The interdigitated piezoceramic is a special case of the aforementioned stacked actuators. The energy expressions are needed to compare the actuation capabilities of the piezoceramic with interdigitated electrodes to those of a piezoceramic with face-plane (conventional) electrodes.

Taking advantage of the symmetry of the interdigitated pattern, one first considers a section of the piezoceramic including one electrode of each polarity (Figure 3.3.) Furthermore, since the thickness of the section is small with respect to the spacing between the electrodes, the transverse component of the electric field is neglected and an average value of the longitudinal component will be considered. The electric potential at all points under an electrode is equal to that of the electrode; therefore, no electric field is considered in these areas. Hence, the average electric field through a section lies in the area between the electrodes and is given by $E = \frac{V}{g}$ where V is the applied voltage to the electrodes and g is the distance between electrodes of opposite polarity.

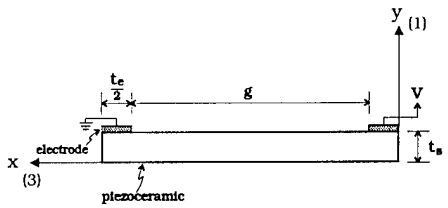

Figure 3.3: A section of the interdigitated-electrode piezoceramic.

The assumptions made here reduce the piezoceramic with interdigitated electrodes to a stack of identical piezoceramic sections with each section as shown in Fig 3.3. Therefore, the results of Section 3.2 are applicable here.

Since thin piezoceramic sections are of main interest, the dominant strain is in the 3-direction (along the length); therefore, from Eq. (3.12) the actuation energy of each section is given by

$$W_{act} = \frac{V w_s t_s e_{33}}{2g} \int_a^{a+g} S_3 dx \tag{3.27}$$

where w_s and t_s are the width and thickness of the piezoceramic section and a and $a+g$ are the spatial limits of the section along the x-axis. The expression for the potential energy, kinetic energy, and force generated by N piezoceramic sections is as given in Eqs. (3.9), (3.10), and (3.24), respectively, with A_p replaced by $w_s t_s$.

To compare the actuation level of a piezoceramic with interdigitated electrodes to those of a conventional piezoceramic plate with face plane electrodes, consider two piezoceramic plates with the same length, width and thickness, l_p, w_p, and t_p, respectively. In the case of the interdigitated piezoceramic, the dominant strain is in the 3-direction whereas the dominant strain of the conventional piezoceramic is in the 1-direction. Comparing the actuation of the proposed piezoceramics yields

$$\frac{W_{act_i}}{W_{act_c}} = \frac{\frac{V w_s t_s}{2g} \sum_{i=1}^{N} \int_{a_i}^{a_i+g} e_{33} S_3}{\frac{V w_p t_p}{2t_p} \int_a^{a+l_p} e_{31} S_1} \tag{3.28}$$

where W_{act_i} is the actuation level of the ceramic with interdigitated electrodes, W_{act_c} is the capability of the conventional piezoceramic, N is the number of section in the interdigitated piezoceramic, and a_i is the spatial limit of the i^{th} piezoceramic section. Normalizing electric fields and taking $t_p = 2t_s$ simplifies the expression into

$$\frac{W_{act_i}}{W_{act_c}} = \frac{w_s e_{33} \sum_{i=1}^{N} \int_{a_i}^{a_i+g} S_3}{2 w_p e_{31} \int_a^{a+l_p} S_1} . \tag{3.29}$$

Similarly, comparing the forces resulting from both ceramics yields

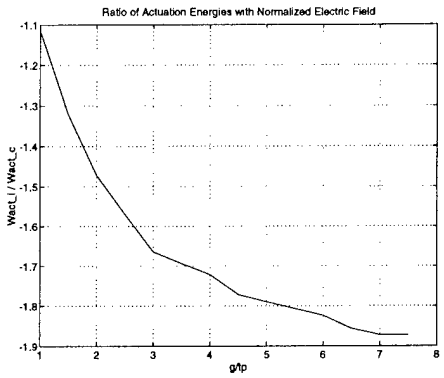

Figure 3.4: Comparison of actuation levels due to conventional and interdigitated piezoceramics.

$$\frac{F_i}{F_c} = \frac{N w_s t_s E e_{33}}{w_p t_p E e_{31}} \tag{3.30}$$

where F_i is the force exerted by the interdigitated piezoceramic and F_c is the force due to the conventional piezoceramic. Note that for a normalized field and $t_p = 2t_s$, the ratio simplifies to

$$\frac{F_i}{F_c} = \frac{N w_s e_{33}}{2 w_p e_{31}}. \tag{3.31}$$

To compare the performance in vibration damping of the two proposed piezoceramic plates, attach each of them to an identical clamped-free beam at identical positions. Fix the width t_e of the fingers of the interdigitated electrodes and let $t_e = t_p$. The actuation energies of the two piezoceramic plates are compared using Eq. (3.29) and the mode shape functions of the clamped-free beam (normalized electric field). Figure 3.4 shows the ratio W_{act_i}/W_{act_c} for different values of g/t_e.

3.4 Wiener-Hopf Design

An analytical solution to the tradeoffs of performance versus stability margin has been attained and reported in [20] (in these proceedings). The approach is based on H_2 measures of performance and stability margin. Furthermore, a novel approach is also introduced which allows structured perturbations in the coprime polynomial matrix fraction description of the plant transfer matrix to be taken into account. The reader is referred to [20] for details.

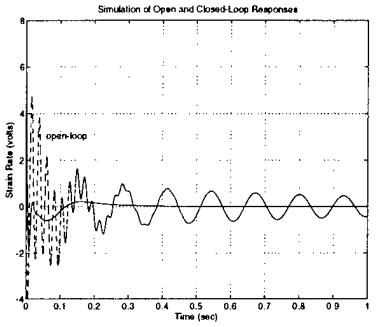

Figure 3.5: Simulation results for open and closed-loop system.

3.5 Simulation and Experimental Results

An interdigitated electrode pattern was deposited onto each side of a PZT, $Pb(Zr,TI)O_3$, plate. The PZT plate was of type 5H, manufactured by Morgan Matroc, Inc. The electrodes were deposited onto the PZT by evaporation. First, the area which was to remain unelectroded was covered with a stainless steel mask. We assured that the electrodes on both sides of the PZT plate were aligned through a registration scheme. Thereafter, a layer of nickel was deposited on each side of the ceramic; nickel provided a strong bond to the ceramic whereas the conductivity of the resulting electrode was not sufficient. To improve the conductivity of the electrodes, a layer of gold was deposited over the nickel resulting in a maximum resistance of 15 Ohms along any pair of electrodes. Electrical contact was established through the use of a two part conductive glue.

A controller based on the Wiener-Hopf (H_2) design methodology is designed for a clamped-free beam with an interdigitated piezoceramic actuator and a conventional piezoceramic sensor. Perfect bonding between the piezoceramic actuator ($2.5'' \times 1.5'' \times 0.020''$) and the rectangular aluminum beam ($17'' \times 5'' \times 1/16''$) is assumed, so that the overall model is not affected by the adhesive layer. The sensor is mounted further above the actuator and due to its non-collocation with the actuator, a non-minimum phase plant is attained. The analytical modeling and the experimental results do match with each other. The parameters in the Wiener-Hopf design were chosen such that the advocated controller was not proper. The controller has four zeros and three poles. This was done in order to achieve velocity feedback for a better active damping of the structure. The controller is as follows:

$$C_w(s) = -\frac{0.188s^4 + 63.56s^3 + 3754.7s^2 + 387420s + 3560400}{s^3 + 171.1s^2 + 4997.7s + 11452}. \tag{3.32}$$

The open and closed-loop responses of the structure for an impulse type force disturbance at the tip of the beam is shown in Fig. 3.5. The applied electric field does not exceed 15 $Kvolts/in.$

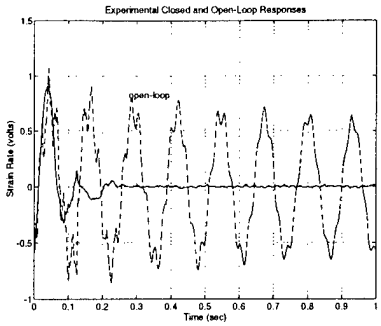

Figure 3.6: Experimental open and closed-loop responses.

The obtained controller was tested on the experimental setup at the CRRL. The controller was discretized and implemented by a '486 based PC with a sampling period of 2 *msec.* The DAC output was filtered with a second-order filter having a natural frequency of 150 Hz. A high voltage amplifie was used to step up the control voltage to the piezoceramic actuator. The open and closed-loop responses are shown in Fig.3.6. A significant improvement in the settling time of the system has been achieved. We are currently implementing controllers on a flexible pointing system.

3.6 Conclusions

Dynamical models of stacked piezoceramic actuators were established. The standard piezoceramic stack actuators and the interdigitated electrode patterns were considered. The stacked piezoceramics were utilized for active structural damping. A new robust control design methodology based on H_2 design was advocated and shown to be an effective design methodology.

3.7 References

[1] N. W. Hagood and A. Von Flotow, "Damping of structural vibrations with piezoelectric materials and passive electrical networks," *Journal of Sound and Vibrations*, vol. 146, no. 2, pp. 243–268, 1991.

[2] F. Khorrami and E. Tome, "Active control of flexible structures with embedded piezoceramics," in *Proceedings of the 1992 IEEE Regional Control Conference*, (Brooklyn, NY), pp. 33–36, July 1992.

[3] F. Khorrami and I. Zeinoun, "Rapid slewing and pointing of a flexible structure with embedded piezoceramics," in *Proceedings of the Conference on Smart Structures and Materials*, (Albuquerque, New Mexico), pp. 25–36, Feb. 1993.

[4] F. Khorrami, I. Zeinoun, and E. Tome, "Experimental results on active control of flexible-link manipulators with embedded piezoceramics," in *Proceedings of*

the 1993 IEEE International Conference on Robotics & Automation, (Atlanta, GA), pp. (3) 222–228, May 1993.

[5] A. J. Bronowicki, J. W. Innis, R. S. Betros, and S. P. Kuritz, "Acesa active member damping performance," in *Proceedings of the Conference on Smart Structures and Materials*, (Albuquerque, New Mexico), pp. 836–847, Feb. 1993.

[6] J. J. Dosch, D. J. Inman, and E. Garcia, "A self-sensing piezoelectric actuator for collocated control," *J. of Intell. Mater. Syst. and Struct.*, vol. 3, pp. 166–185, Jan. 1992.

[7] I. Zeinoun and F. Khorrami, "An adaptive control scheme based on fuzzy logic and its application to smart structures," *Journal of Smart Materials and Structures*, vol. 3, no. 3, pp. 266–276, 1994.

[8] S. Takahashi, "Longitudinal mode multilayer piezoceramic actuators," *Ceramic Bulletin*, vol. 65, no. 8, pp. 1156–1157, 1986.

[9] N. Hagood, R. Kindel, and K. Ghandi, "Improving transverse actuation of piezoceramics using interdigitated surface electrodes," *Smart Structures adn Intelligent Systems*, vol. 1917, pp. 341–352, 1993.

[10] J. J. Bongiorno, Jr., F. Khorrami, and T. Lin, "A Wiener-Hopf approach to tradeoffs between stability margin and performance in two and three-degree-of-freedom multivariable control systems," in *Proceedings of the American Control Conference*, (Seattle, WA), June 1995.

4. Publications and Technical Reports for this Grant

- Refereed Journal Papers (appeared, accepted, and submitted)

[1] S. Jain and F. Khorrami, "Robust adaptive control of flexible joint manipulators." *Automatica.* (To appear).

[2] F. Khorrami, J. Lewinsohn, J. Rastegar, and S. Jain, "Feedforward control for vibration free maneuvers of flexible manipulators via the Trajectory Pattern Method." *IEEE Trans. on Control Systems Technology.* (Accepted pending revision).

[3] S. Jain and F. Khorrami, "Decentralized adaptive output feedback Design for large scale nonlinear systems." *IEEE Trans. on Automatic Control*, vol. 42, no. 5, pp. 729-735, May 1997.

[4] S. Jain and F. Khorrami, "Robust decentralized control of power systems utilizing only swing angle measurements." *International Journal of Control*, vol. 66, no. 4, pp. 581-601, March 1997.

[5] S. Jain and F. Khorrami, "Decentralized adaptive control of a class of large scale interconnected nonlinear systems," *IEEE Trans. on Automatic Control*, vol. 42, no. 2, pp. 136-154, Feb. 1997.

[6] S. Jain, F. Khorrami, and B. Fardanesh, "Decentralized control of large-scale power systems with unknown interconnections," *International Journal of Control*, vol. 63, no. 3, pp. 591-608, Feb. 1996.

[7] S. Jain and F. Khorrami, "Positioning of unknown flexible payloads for robotic arms using a wrist-mounted force/torque sensor," *IEEE Trans. on Control Systems Technology*, vol. 3, no. 2, pp. 189-201, June 1995.

[8] I. J. Zeinoun and F. Khorrami, "An adaptive control scheme based on fuzzy logic and its application to smart structures," *Journal of Smart Materials and Structures*, vol. 3, no. 3, pp. 266-276, 1994.

- Refereed Conference Papers (appeared, accepted, and submitted)

[9] H. Melkote and F. Khorrami, "Robust adaptive control of direct drive brushless DC motors and applications to robotic manipulators," in *Proceedings of the 1997 IEEE Conference on Control Applications*, (Hartford, Connecticut), August 1997. (To appear).

[10] H. Melkote and F. Khorrami, "Robust adaptive control oí permanent magnet stepper motors," in *Proceedings of the 1997 European Control Conference*, (Brussels, Belgium), July 1997.

[11] H. Melkote, F. Khorrami, S. Jain, and M. Mattice, "Adaptive nonlinear control of variable reluctance stepper motors," in *Proceedings of the 1996 IEEE Conference on Decision and Control*, (Kobe, Japan), Dec. 1996.

[12] S. Jain and F. Khorrami, "Application of a decentralized adaptive output feedback based on backstepping to power systems," in *Proceedings of the 34th IEEE Conference on Decision and Control*, (New Orleans, Louisiana), pp. 1585-1590, Dec. 1995.

[13] F. Khorrami, J. Rastegar, and S. Jain, "Inversion of flexible manipulator dynamics via the Trajectory Pattern Method," in *Proceedings of the IEEE Conference on Decision and Control*, (New Orleans, Louisiana), pp. 3325-3330, Dec. 1995.

[14] S. Jain and F. Khorrami, "Robust adaptive control of nonlinear systems with application to flexible joint manipulators." in *Proceedings of the 34th IEEE Conference on Decision and Control*, (New Orleans, Louisiana), pp. 2829-2834, Dec. 1995.

[15] F. Khorrami and J. Rastegar, "Simultaneous structure and control design for a flexible weapon pointing system actuated by active materials," in *Proceedings of the 34th IEEE Conference on Decision and Control*, (New Orleans, Louisiana), pp. 4374-4379, Dec. 1995.

[16] S. Jain and F. Khorrami, "Decentralized Control of Large Scale Power Systems with Unknown Interconnections," in *Proceedings of the IEEE Conference on Control Applications*, (New Albany, New York), pp. 618-623, Sept. 1995.

[17] [1] S. Jain and F. Khorrami, "Robust adaptive control of a class of nonlinear systems: state and output feedback," in *Proceedings of the American Control Conference*, (Seattle, Washington), pp. 1580-84, June, 1995.

[18] S. Jain and F. Khorrami, "Decentralized adaptive control of a class of large scale interconnected nonlinear systems," in *Proceedings of the American Control Conference*, (Seattle, Washington), pp. 2938-2942, June, 1995.

[19] S. Jain and F. Khorrami, "Decentralized adaptive output feedback control of large scale interconnected nonlinear systems," in *Proceedings of the American Control Conference*, (Seattle, Washington), pp. 1600-1604, June, 1995.

[20] F. Khorrami, I. Zeinoun, J. J. Bongiorno, and S. Nourbakhsh, "Application of H_2 Design for vibration damping and pointing of flexible structures with embedded

[1] This report was one of the five finalists chosen for the 1995 ACC Best Student Paper Award.

smart materials," in *Proceedings of the American Control Conference*, (Seattle, Washington), pp. 4178-4182, June, 1995.

[21] S. Jain and F. Khorrami, "Decentralized adaptive control of mismatched large scale interconnected nonlinear systems," in *Proceedings of the Symposium Nonlinear Control Systems Design*, (Tahoe City, CA), pp. 314-319, June, 1995.

[22] F. Khorrami, "Adaptive nonlinear control for end-effector position tracking of multi-link flexible manipulators with embedded active materials," in *Proceedings of the 33rd Conference on Decision and Control*, (Orlando, Florida), pp. 103-108, Dec. 1994.

[23] J. Rastegar, F. Khorrami, and Z. Retchkiman, "Inversion of nonlinear systems via trajectory pattern method," in *Proceedings of the 33rd Conference on Decision and Control*, (Orlando, Florida), pp. 2382-2387, Dec. 1994.

[24] F. Khorrami, "Adaptive control of flexible-link manipulators with piezoelectric ceramic sensors and actuators," in Proceedings of the *IFAC Symposium on Robot Control*, (Capri, Italy), pp. 593-598, Sept. 1994.

[25] I. Zeinoun and F. Khorrami, "An adaptive fuzzy based controller and its application to smart structures," in *Proceedings of the American Control Conference*, (Baltimore, Maryland), pp. 575-579, June 1994.

[26] F. Khorrami and I. Zeinoun, "Fuzzy-neural network based controls for smart structures with piezoceramics sensors and actuators." in *Proceedings of the Smart Structures and Materials Conference*, (Orlando, Florida), pp. 684-695, Feb. 1994.

5. Personnel and Students Supported by this Grant

Professors Khorrami (PI) and Pillai and Nourbakhsh (Co-PIs) were supported by this grant. Furthermore, the following students were partially supported on this research grant:

- Sandeep Jain; attained his M.S. and Ph.D. degress in the Electrical Engineering.
- Hemant Melkote; attained the M.S. degree in the Electrical Engineering and is currently continuing for his Ph.D.
- Sivakumar Sankaranarayanan; attained his M.S. degree in the Electrical Engineering and is currently pursuing his Ph.D. degree.
- Issam Zeinoun; attained his M.S. degree in the Electrical Engineering and is currently pursuing his Ph.D.